Contents

1. Background 4
1.1 Introduction 4
1.2 Flexible displays 5
1.2.1 The current state of flexible displays 5
1.2.2 Display technology options 5
1.2.3 Device structure 6
1.3 Conducting transparent flexible layers 7
1.3.1 Properties of indium tin oxide 7
1.3.2 Alternative conducting transparent flexible layers 8
1.3.3 Substrates 8
1.4 Mechanical failure of ITO polymer layers 9
1.4.1 Crack onset strain 9
1.4.2 Cracking model 10
1.5 Corrosion of ITO polymer layers 11
1.5.1 Mechanism of ITO corrosion 11
1.5.2 The effect of acrylic acid on ITO polymer layers 12
1.6 Combined mechanical and corrosive failure 13
1.6.1 Mechanism of failure under combined stress and corrosion 13
1.7 Cyclical loading 15
1.7.1 The effects of cyclical loading on ITO polymer systems 15
1.8 Wear of ITO polymer layers 17
1.8.1 Dry wear 17
1.8.2 Wet wear 18
1.8.3 Nanoscale wear properties 18
1.9 Production of ITO polymer layers 19
1.9.1 Magnetron sputtering 19
1.9.2 Sol-gel production 20
1.9.3 Pulsed laser deposition 20
1.9.4 Inducing crystallinity in samples by changing deposition temperature 22

2 Aims and objectives 24
2.1 Scope of the project 24
2.2 Sample production 24
2.3 Sample characterisation 24
2.3.1 Strain behaviour 24
2.3.2 Wear behaviour 25
2.3.3 Surface roughness 25
2.3.4 Crystallinity 25
3 Experimental method 26
3.1 Sample production 26
3.1.1 Substrate preparation 26
3.1.2 ITO deposition by PLD 26
3.1.3 ITO deposition by magnetron sputtering 27
3.2 Sample characterisation 27
3.2.1 Tensile testing with simultaneous resistance measurement 27
3.2.2 Acid immersion 28
3.2.3 X-Ray diffraction 29
3.2.4 SEM analysis 29
3.2.5 TEM analysis 30
3.2.6 Atomic force microscopy for surface roughness measurement 30
3.2.7 Fragmentation analysis 31
3.2.8 Nanoscratching 31
4 Results and Discussion 34
4.1 ITO on PET 34
4.2 ITO on PEN 35
4.2.1 SEM images 36
4.2.2 ITO on PEN resistance data 40
4.2.3 Fragmentation analysis 46
4.2.4 XRD data 49
4.2.5AFM surface roughness 49
4.2.6 TEM analysis for crystallinity 51
4.3 Commercial Samples 53

4.4 Nanoscratching 55
5 Conclusions 56
5.1 Conclusions 56
5.2 Future work 57

1. Background

1.1 Introduction

Over the last 10 years, liquid crystal display (LCD) and plasma screens have all but replaced traditional cathode ray tube (CRT) screens, in both domestic and industrial markets (Sang Soo 2008). This is mainly due to their decreased size and weight, rendering them portable and less intrusive as a display unit. Flexible screens promise to revolutionise the display industry in a similar way, with the introduction of lighter and more compact units, with advantages in adaptability, customisation and manufacturing techniques (Raupp 2008). Manufacturing costs could be driven down dramatically due to the possibility of roll-to-roll processing (McCollough, Rankin *et al.* 2005). Flexible displays are characterised by the use of polymer rather than glass substrates and range from slightly flexible to fully rollable like a sheet of cloth (Crawford 2005).

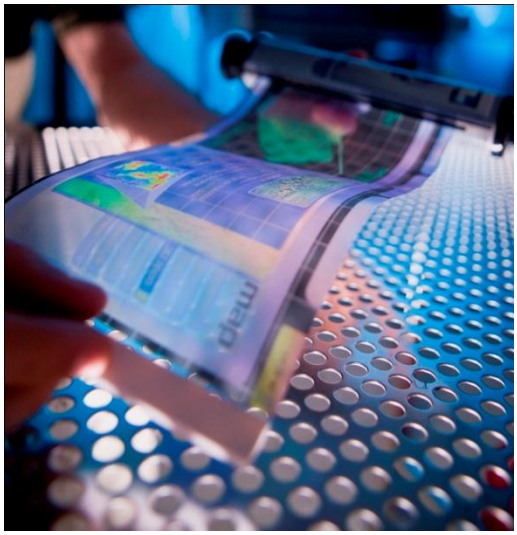

Figure 1. Prototype flexible display created at Arizona State University's Flexible Display. ASU Flexible Display centre brochure, Nick Colaneri, 2010

Flexible displays have several highly useful potential applications. There is significant military interest as they are not brittle like glass-based displays, so will be much more robust and resistant to shock on the

battlefield (Morton, Forsythe *et al.* 2007). For personal use, they may be rolled up and only have a small volume for transportation, but be unrolled at the point of use and give a large information display area. They may also be affixed to curved surfaces such as windscreens, enabling the use of electronic displays in applications where they may before have been unsuitable (Crawford 2005).

1.2 Flexible displays

1.2.1 The current state of flexible displays

Several large electronic manufacturers have already developed, tested and produced e-paper style displays (Allan 2006). These displays use electronically actuated e-ink, which is similar to paper in that it does not illuminate itself but rather reflects ambient light. As there is no illumination the power requirements are very low; it does not need constant refreshing (again, causing less power to be consumed) and the viewing angle is high (Hayes 2009).

Although e-paper is a good starting point for flexible displays, it is clear that to become widely used and supersede conventional displays, manufacturers must be able to produce high-resolution, colour and video screens with a flexible touchscreen (Kroeker 2009). Whilst new display technologies must evidently be investigated and improved, the current non-existence of a flexible e-paper display with touchscreen capability indicates that even in mature display technologies there are problems with flexible touchscreens.

1.2.2 Display technology options

With regard to uncommercialised colour and video-capable flexible displays there is a large variety of flexible display technologies currently vying for superiority (dependent on application), such as organic light-emitting diodes (OLEDS) (Shinar and Shinar 2008), polymer-dispersed liquid crystals (Aleksander and Klosowicz 2004) and paintable LCDs (Vogels, Klink *et al.* 2004). These display methods must be flexible themselves, attach to flexible substrates, and most importantly be cheap to produce in bulk.

OLEDs currently seem the most promising as they are cheap and printable, but they have a very short lifetime as they are unstable in the presence of oxygen (Lisong, Wanga *et al.* 2006). When this problem is solved, it seems likely that flexible displays will become widely available to customers in many spheres.

1.2.3 Device structure

Conducting substrates are used as electrodes in many display devices, carrying current to each individual pixel. Capacitive touchscreens similarly require a conductive layer, as they sense the charge of the fingertip determining the position of the finger relative to the display. The touchscreen element must be also transparent so that the display remains visible beneath it. This means that capacitive touchscreen devices require a layer which is simultaneously electrically conductive and optically transparent.

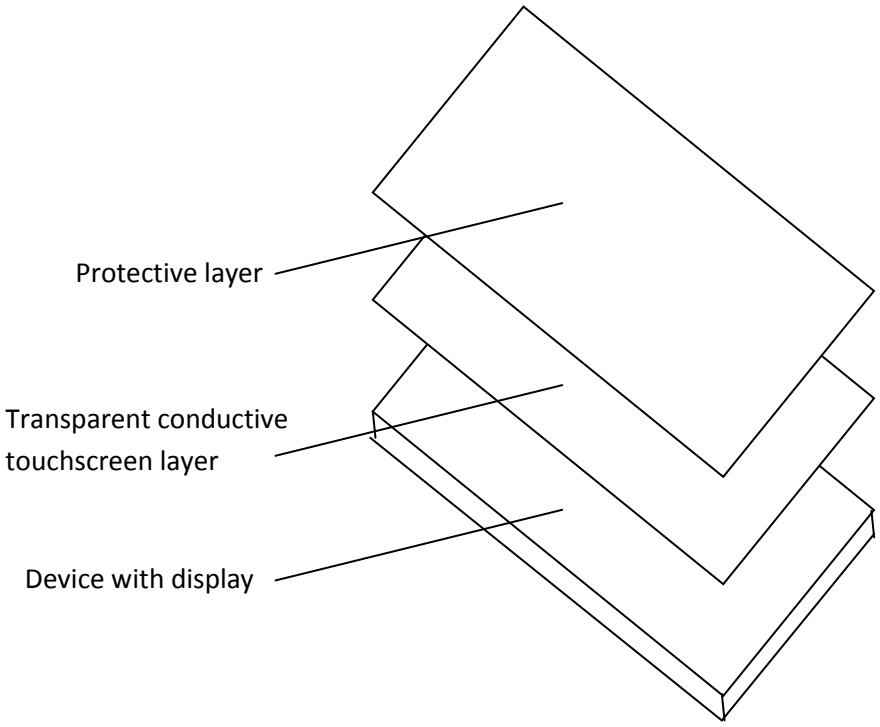

Figure 2. Touchscreen device architecture. In a flexible display, every one of these layers must be flexible whilst maintaining the same functionality.

1.3 Conducting transparent flexible layers

1.3.1 Properties of indium tin oxide

All touchscreen devices require a conducting transparent layer, and indium tin oxide (ITO) is currently being widely used for this purpose on glass substrates (Yip, Gururaj Bhat *et al.* 1994). This ITO on glass system is well researched and understood, but is not flexible as glass is a rigid substrate. Resistivities as low as 6×10^{-4} Ω cm can be achieved with careful sputtering (see section 1.9.1) (Shin, Shin *et al.* 2001), and thin layers of ITO have been shown to have an optical transparency of around 87 % (Kim, Horwitz *et al.* 2001) – high enough for the proposed display applications

ITO films conduct electricity via a tin-doped In_2O_3 lattice. The addition of tin causes the substitution of

Sn4+ for In3+, creating more conduction electrons via the n-type donor mechanism (Hartnagel, Dawar *et al.* 1995). At high levels of Sn content (>10 mol %), n-type doping is the dominant factor in raising conductivity; whilst oxygen vacancies play a role in determining conductivity at lower Sn levels (Kwok, Sun *et al.* 1998). ITO has a coefficient of thermal expansion of 7.2 X 10^{-6} °C^{-1} (Wu and Chiou 1997).

1.3.2 Alternative conducting transparent flexible layers

Alternative transparent conducting layers include zinc oxide (ZnO) and poly(3, 4-ethylenedioxythiophene) poly(styrenesulfonate**)**(PEDOT:PSS). Zinc oxide, heavily doped with aluminium, has been used commercially for many years as the transparent electrode in solar cells (Weigel and Dreyer 2008), and can have resistivities as low as 1.4 x 10^{-4} Ω cm (Ellmer 2001) i.e. better than ITO. It also has a comparable optical transmittance of approximately 85% (Yang and Zeng 2009). However, it is unlikely to be used instead of ITO currently, as it is similarly susceptible to cracking and has not historically been as widely used for display applications. PEDOT:PSS has the advantage of being much more flexible than ITO (Lang, Naujoks *et al.* 2009), so cracking will not be a problem if the film is subjected to bending strains. Unfortunately, PEDOT:PSS is considerably less conductive than both ITO and ZnO, and the lowest resistivities found in commercial samples are in the region 0.15 Ω cm (Sankir 2008). Although its mechanical properties are ideal for flexible displays, it would not be able to provide the current required to power a display.

1.3.3 Substrates

Conducting transparent layers must be attached to a flexible transparent substrate, of which polymers are the ideal and obvious candidate. PET (polyethylene tetrephthalate) and PEN (polyethylene naphthalate) have previously been selected and extensively studied for this application (Cho, Choi *et al.* 2008; Seo, Kang *et al.* 2009; Cao, Chen *et al.* 2009; Hauk and Alford 2007; Heusing, Oliveira *et al.* 2008) as they show suitable mechanical properties. PET has a T_g (glass transition temperature) of 69 – 115 °C,

has a tensile modulus of approximately 1.7 GPa (relatively stiff), a coefficient of thermal expansion of 16 x 10^{-6} °C^{-1} (Ma, Bhushan, 2003) and has reasonable gas barrier properties (Mark 2009). PET is often used for drinks bottle containers, and is a widely used, cheap and readily available material. PEN is a stiffer polymer with a modulus of approximately 2 GPa, a coefficient of thermal expansion of 8 x 10^{-6} °C^{-1} (Ma, Bhushan, 2003) and has a T_g of 137.5 °C(Mark 2009). Both can be purchased in heat stabilised varieties, and have similar tensile strengths. The fact that these polymers are only dimensionally stable up to a maximum of 150 °C limits the processing parameters for ITO deposition. Films grown on polymeric substrates tend to have a slightly higher resistivity and lower optical transmittance than those grown on glass (Shin, Shin *et al.* 2001), but the difference in properties caused by substrate choice is negligible.

1.4 Mechanical failure of ITO polymer layers

1.4.1 Crack onset strain

Although there are myriad factors including electronic, optical transmission and substrate issues that could cause the failure of ITO-polymer films in device structures, Chen *et al.* (Chen *et al.* 2008) have noted the fact that ITO failure by cracking is the main impediment to flexible touchscreens. When the high-modulus ITO adheres to the flexible substrate there is a significant modulus mismatch which can cause cracking of the ITO layer and reduce its conductivity (Cairns and Crawford 2005). Thicker layers provide greater conduction, but they also increase the strain on the ITO layer and accelerate cracking (Leterrier, Medico *et al.* 2004), so a balance must be found. Experimental results have shown that a layer 100 nm thick will provide acceptable levels of both conductance and flexibility, and can give a radius of curvature of up to 1 cm (500 – 700 MPa bending strain) before conductivity is lost (Zhinong, Yuqiong *et al.* 2009). A commonly-used comparative measure of resistivity is the crack onset strain (COS), when resistance has increased by 10 % (Cairns, Sachsman *et al.* 2000). The COS shows when the resistivity has begun to increase as cracks have been initiated and prevent normal conduction of electrons. The COS varies depending on deposition conditions and method, but has an average of 2-2.5%

for a 100 nm ITO layer on PET under uniaxial tension - shown in Figure 3 as the point at which resistance starts to increase sharply (Caims, Witte *et al.* 2000). Tensile strain is measured as the ratio of change in length to initial length ($= \Delta L/L_0$ where ε is the tensile strain, ΔL is the change in length, L_0 is the initial length).

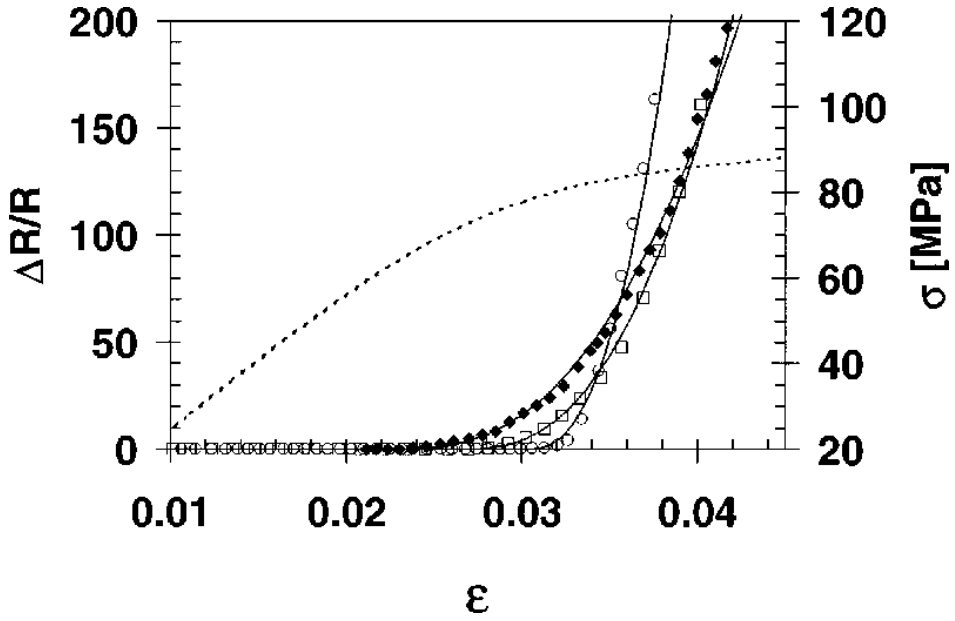

Figure 3. Change in resistance against strain for different thicknesses of ITO on a PET substrate (Cairns and Crawford 2005).

1.4.2 Cracking model

Cracks in ITO on a PET substrate are commonly modelled by the Kelly-Tyson approach (Kelly and Tyson 1965). Cairns (Caims, Witte *et al.* 2000) and Leterrier (Leterrier, Boogh *et al.* 1997) have experimentally supported the applicability of this model. The Kelly-Tyson approach is used to model the behaviour of brittle films on flexible substrates, which accurately sums up the ITO-polymer system. This model tells us that at each crack there is a large non-conducting gap between the two sides of the ITO layer, but there is a small conducting interfacial layer bridging it as seen in Figure 4. The exact composition and nature of this interface is not known, but Cairns assumes it to be a combination of ITO and the polymer. As strain increases the width of the crack increases, and new cracks will nucleate and grow. In uniaxial tension,

initially transverse cracks will propagate perpendicular to the direction of straining, which are assumed to account for the initial drop in conductivity. Secondarily, there will also be cracking or delamination due to the lateral contraction mismatch between the substrate and the conducting film (Kim, Yang *et al.* 2010).

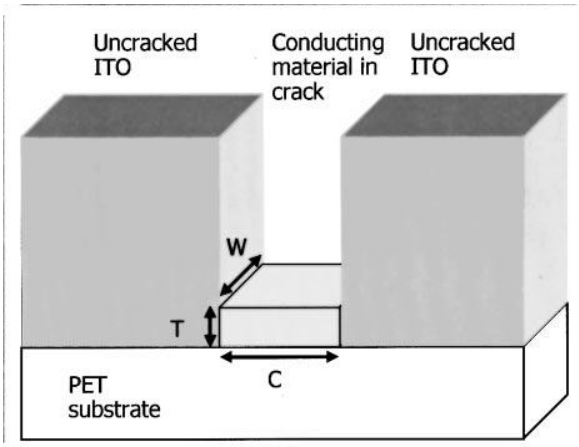

Figure 4. Bridging material which rests between cracks on a strained ITO-PET sample (Caims, Witte *et al.* 2000).

Resistivity decreases gradually because the ductile interfacial material bridging the cracks is only slightly conductive (as it is not purely ITO), and gradually becomes the dominant conductor. Resistivity stops decreasing and levels out when crack saturation is reached; or when conductivity decreases to zero, before crack saturation is reached.

1.5 Corrosion of ITO polymer layers

1.5.1 Mechanism of ITO corrosion

ITO clearly loses functionality when excessively stressed (either in compression, tension or bending), but the presence of acids may exacerbate this, either by increasing the rate of crack growth or decreasing the strain required to initiate cracks. This process is known as stress corrosion cracking (SCC), and can cause the premature loss of functionality in ITO components. ITO coatings are known to corrode as they often need patterning, which can be achieved by selective etching with corrosive acids. Folcher *et al.*

(Folcher, Cachet *et al.* 1997)demonstrated that certain solutions will corrode ITO layers effectively and quickly, by measuring changes in mass and current when ITO films are exposed to electrolytes of HCl and $LiClO_4$. When the potential is positive enough for chloride ions to be oxidised into radical species, these radical species attack the indium-oxygen bonds. Figure 5 shows that this attack happens primarily at grain boundaries in polycrystalline ITO (Folcher, Cachet *et al.* 1997).

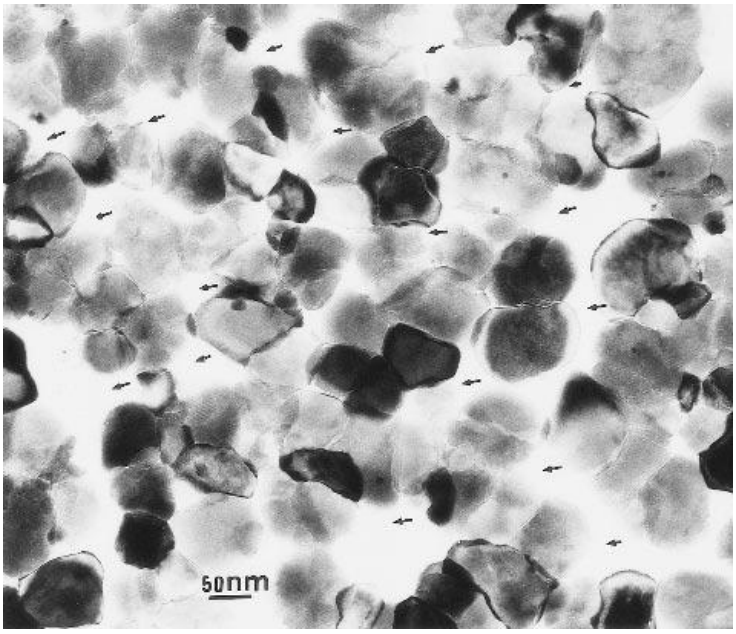

Figure 5.TEM image of ITO on a glass substrate after being subjected to acidic attack by HCl. The arrows indicate areas which were subjected to the most aggressive intergranular attack (Folcher, Cachet *et al.* 1997),

1.5.2 The effect of acrylic acid on ITO polymer layers

It is unlikely that HCl or $LiClO_4$ solutions will be found in the device structures proposed for flexible ITO-based screens, but other acids may be present and in contact with the ITO film. Acrylic acid is one possible candidate, as acrylic acid containing adhesives can degrade ITO films (Sierros, Morris *et al.* 2009). Morris *et al.* (Morris, Sierros *et al.* 2008) immersed ITO on PET samples in varying concentrations of acrylic acid for different lengths of time, and measured the change in resistance. It was found that the resistance gradually decreased over time during immersion, indicating that corrosion of the ITO was occurring. The samples immersed in 0.5 to 0.9 Mol/L acid showed a decrease to zero conductivity within

a few minutes, whilst those immersed at 0.1 Mol/L acid took around 30 hours for the same change (Figure 6). Corrosion was found to occur mostly at areas of high surface roughness, due to an increased surface area. The effects of corrosion can be mitigated by decreasing the surface roughness of the film by using smooth substrates or different processing parameters, as discussed later. The exact mechanism of corrosion of ITO by acrylic acid is not noted in this work, nor appears to have been published elsewhere, suggesting that it is not currently known. It is reasonable to assume that the In-O bonds are broken during the corrosion process, as in the corrosion of ITO by radical species from an HCl solution.

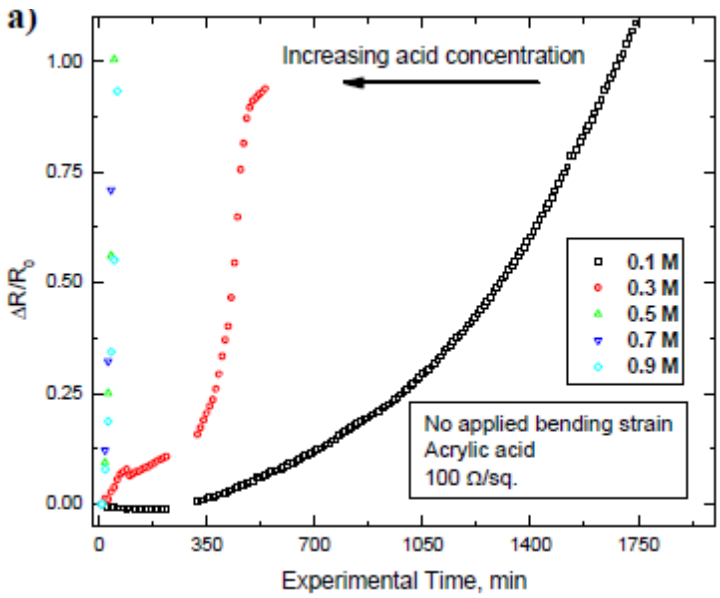

Figure 6. Change in resistance against experimental time for samples of ITO on PET. (Morris, Sierros *et al.* 2008).

1.6 Combined mechanical and corrosive failure

1.6.1 Mechanism of failure under combined stress and corrosion

Stress corrosion cracking (SCC) occurs when strain is applied in the presence of a corroding substance. In a situation where this is occurring, both effects are likely to exacerbate each other (Jones 1992). Stress corrosion cracking is also a very local phenomenon, and the main surface of the material may be undamaged. However, as the crack propagates a crevice may appear, in which the pH of the acid will steadily rise as corrosion occurs, due to a lack of mixing with more dilute acid from outside of the

crevice (Jones 1992). This can lead to high acid concentrations in the crevice as well as high stress concentrations at the crack tip, which further enhances the severity of the cracking. In ITO thin films, the cause of SCC failure is the presence of a network of a large number of small cracks rather than one critical crack (Cairns and Crawford 2005), but localised acid concentrations and stress concentrations may still play a large role in failure. Ramji *et al* (Ramji, Cairns *et al.* 2007) showed that the cracks which occur in patterned ITO/PET sheets initiate on microcracks present from the patterning process and are up to seven times worse on patterned samples which have microcrack initiation sites.

Sierros *et al* (Sierros, Morris *et al.* 2009) developed this work by studying the effects of applied strain in conjunction with the presence of acrylic acid (0.1 – 0.9M concentration). It was found the presence of acid can cause cracks to initiate at strains as low as a quarter of those seen in uncorroded samples, indicating that SCC is indeed occurring. Some preliminary work by Ellis (Ellis 2009) confirmed that the presence of 0.1M acrylic acid did cause corrosion, but found that COS occurred at the same point for both corroded and non-corroded samples, and the presence of acid only caused a rate of resistance increase after the COS was exceeded. Acrylic acid was used as it is the acid which the samples would experience in use, as acrylate inks and adhesives are used in flexible display devices. Sierros *et al* (Sierros, Morris *et al.* 2009) concluded that corrosion was the dominating factor in this mechanism rather than stress. They also found that the corrosion was most prevalent at regions of high surface roughness, where a large surface area is exposed to the acid, and the presence of crevices for increased acid concentration is most likely.

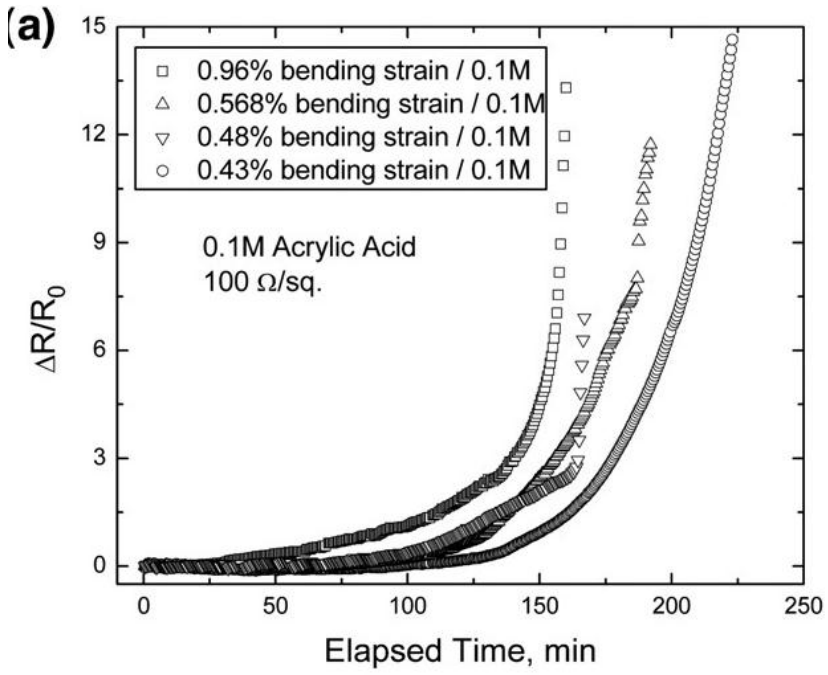

Figure 7. Change in resistance against experimental time for samples of ITO on PET (Sierros, Morris *et al.* 2009).

Morris also conducted work in this field, and SEM analysis again found corrosion to be the dominant factor causing failure, with bending strains assisting (Morris, Sierros *et al.* 2008). Bending strain is a measure of the ratio of distance from the neutral axis to the radius of curvature ($\varepsilon_b = \frac{y}{\rho}$ where ε_b is the bending strain, y is the distance from the neutral axis and ρ is the radius of curvature). They focus on a constant bending strain being applied during immersion, as the sample is wrapped around a mandrel for the duration of the experiment. Some samples were corroded for up to 1000 minutes in 1 M acid, and in these cases SEM images showed the polymer substrate underneath, indicating that all the ITO had been stripped away.

1.7 Cyclical loading

1.7.1 The effects of cyclical loading on ITO polymer systems

Another problem which flexible thin films are certain to face is the application of cyclic loads. Processes such as rolling and unrolling a screen, or repeated bending under touch-screen use will cause repeated

strains and strain reversals. As these processes will be within normal use of the screen, the strains used will be less than the failure strains of the system. However, it is likely that large numbers of these strain reversals could eventually cause failure of the system, as shown by Cairns' (Cairns, Paine *et al.* 2001) work simulating pen strokes on a touchscreen. In this situation, substrate deformation was the cause of failure as it led to delamination of the ITO, and so cracking, all at strains below the COS. Work by Lechat (Lechat, Bunsell *et al.* 2006) confirms that PET fibres undergoing cyclic loading will fail at low stresses, and that they will fail via a step by step crack propagation mechanism

Gorkhali and Cairns (Gorkhali, Cairns *et al.* 2004) furthered these cyclic loading experiments by simulating rolling-unrolling strain reversals (Figure 8). An ITO-PET sheet was repeatedly rolled and unrolled around mandrels of varying diameters to between 0.6 and 2% strain whilst the resistance was continuously measured. It was found that up to between 50-100 cycles there was an increase in resistance due to sample dimension changes, as the PET reached dimensional equilibrium. Once the system was stable there was then a slow increase in resistance over time up to approximately 50,000 cycles, which was found to be due to cracking of the ITO layer whilst strain remained constant. After this point severe cracks occurred, causing catastrophic failure. A polymeric conducting film of polyethylenedioxythiophene, doped with polystyrene sulfonate (PEDOT:PSS), was also investigated, and found to respond much better to cyclic loading, with minimal resistance increase. PEDOT:PSS does however have a higher initial resistance than ITO-PET. The effect of acid on cycling loading has not been investigated, but as it would cause the ITO to crack earlier, it seems likely that it would shorten the fatigue life of similar components.

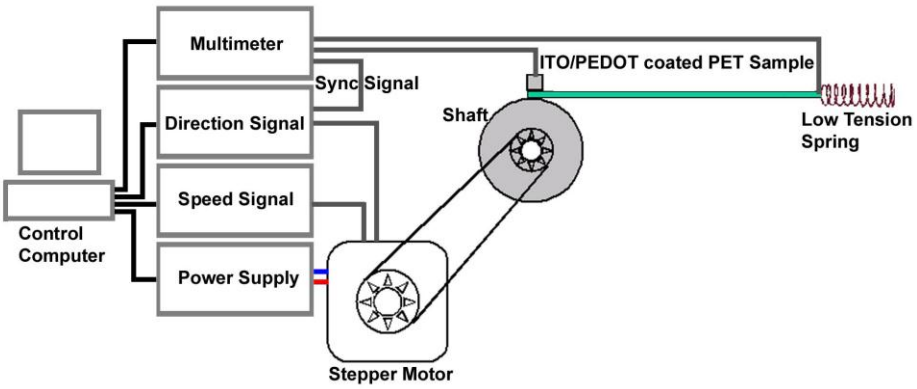

Figure 8. Experimental apparatus for cyclic loading experiments (Gorkhali, Cairns *et al.* 2004).

1.8 Wear of ITO polymer layers

1.8.1 Dry wear

As well as resistive failure due to cracking caused by strain, ITO films may also be at risk from wear-induced failure. The tribological properties of ITO on PET or PEN are poorly understood and have not been investigated to a great degree, but the films will be subject to wear during manufacture and use. Because the ITO layer is very thin (~200 nm), the tribological properties are often substrate dominated, so it is important to also understand the wear behaviour of uncoated PET and PEN. Sierros and Kukureka (Sierros and Kukureka 2007) conducted ball-on-disc experiments on biaxially-oriented PET and PEN to assess predicted behaviour for display applications, with a normal force of 9.8 N being used. It was found that PEN is smoother and has a higher Knoop hardness than PET, and below 6450 sliding cycles it has a lower wear rate. Above 8000 cycles however, PEN has a slightly higher wear rate than PET. It was also found that two types of debris were produced – small and round, or larger with edges – which can modify wear behaviour, and that PET was subject to microcutting (which directly leads to wear) whilst PEN was not.

Work by Wu (Wu and Chiou 1997) characterised the adhesion strength and scratch resistance of sputtered ITO on glass and polycarbonate (PC) substrates. Whilst this is not directly comparable with

PET or PEN coatings, is does offer an insight into how ITO may wear as a thin film on a flexible substrate. Wu showed that hardness increases as thickness of the ITO film increases. Hardness can be used as an indicator of wear resistance, so thicker films are likely to perform better. It is also shown that pull-off strength of the film is much lower on PC than on glass, indicating that glass has better adhesion to ITO. The scratch tests show that ITO on PC is very susceptible to scratching, and as the normal load of the scratch increases then more cracking is observed parallel to the direction of scratching. Sierros *et al* (Sierros, Morris *et al.* 2009) investigated wear of reciprocating sliding ITO surfaces (on PET substrates) against one another, as might be found in a touchscreen device, and simultaneously measured electrical resistance. At a normal load of 3.5 N they found a sharp resistance increase at 10,000 cycles, and that wear was due to abrasive wear, PET deformation, cohesive failure within film, and adhesive wear between ITO and PET. They also found a relationship between resistive increases and weight loss measurements, indicating that a large amount of ITO is lost from the film during the experiment.

1.8.2 Wet wear

Sierros *et al* also investigated the effects of acrylic acid on reciprocating sliding wear. The experimental procedure was the same as with dry sliding wear, except for the addition of 0.1 M acrylic acid prior to wear testing. It was found that the acrylic acid initially acted a lubricating layer on the ITO, and there was less wear at the start of the process. However, this lubricating effect lasted for only a short amount of time, and the overall effect of the addition of acrylic acid was not clear from this study. No other work appears to have been done on the tribocorrosion of ITO, so the effect of increased acid concentrations or different wear mechanisms such as scratching is unknown.

1.8.3 Nanoscale wear properties

The behaviour of ITO on flexible substrates is always highly affected by the substrate when macroscopic wear tests such as ball-on-disc or reciprocating ITO sheets are used. To understand the wear behaviour

of ITO thin films without substrate effects, it is necessary to look at tribological behaviour on the nanoscale. Nanoindentation and nanoscratching using an AFM are potential candidates as experimental techniques for this, and Tseng (Tseng 2010) has compiled an excellent paper detailing the process and comparing different materials and techniques. Tseng assessed hardness, wear coefficent and scratch ratio as possible candidates for being the best nanoscale scratch-resistance indicator, and found the "scratch ratio" of the scratch penetration depth to threshold force (α_i/F_t) to be the most suitable, linking experimental data well with theoretical predictions. However, wear coefficient and hardness are both very important indicators and should also be considered. Tseng also importantly confirmed the "l*ogarithmic relationship between groove size and applied force* (Figure 9)*, and the power law relationship between groove size and cycles.*" For a silicon surface, normal forces up to 100 µN are used, and cantilevers are diamond tipped with a radius between 15 nm (atomic scratching) and 300 nm.

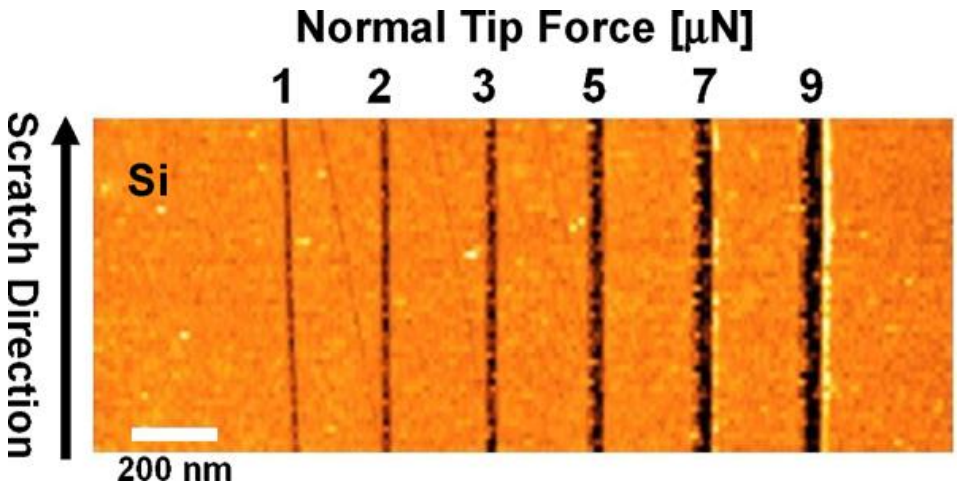

Figure 9. Scratch width of a 120 nm tip radius diamond cantilever on silicon (Tseng 2010).

1.9 Production of ITO polymer layers

1.9.1 Magnetron sputtering

Magnetron sputtering has been used to produce thin films commercially since the 1970s, and there is already a large industry producing magnetron-sputtered ITO films on glass (You, Kim *et al.* 2008), and

more recently, plastics substrates (Anguita, Thwaites *et al.* 2007). Many of the experiments mentioned in this literature survey have used samples produced via magnetron sputtering. Under vacuum a voltage is applied to the ITO target, in conjunction with a strong magnetic field from permanent magnets causing a high density of secondary electrons over the target. Argon atoms are also continuously introduced to the chamber, which are ionised by the electrons and become positively charged above the target. The argon ions are attracted to the negatively charged target, bombard it at high speed and eject target material which is then deposited on the substrate (Zhang and Ali 2007). Careful positioning of the target and the substrate mean that the ejected material is deposited on the substrate. Parameters which can be adjusted to control film properties include target-substrate distance, target composition, electrical current, magnetic field strength, and magnetic field path (Yu, Wang *et al.* 2006). The sputtering process is completed inside a vacuum, and the substrate may be heated during (Thornton 1978) or before deposition.

1.9.2 Sol-gel production

Sol-gel methods are also a prospective deposition route, but the main barrier currently standing in the way is the high post-processing temperatures needed to achieve high-purity films. Essentially, a mix of chemicals containing indium and tin in solvents is prepared, which can be printed (highly useful as it removes the need for an etching process) or otherwise deposited on the substrate(Sakka 2005). This then needs to be dried at approximately 120 °C to remove the solvents, and then annealed, often at temperatures as high as 550 °C (Su, Sheu *et al.* 2005), to produce the desired ITO microstructure. In this way, 200nm thick films can be prepared with optical transmissivities of over 80% and very low surface roughness.

1.9.3 Pulsed laser deposition

Pulsed laser deposition (PLD) can be used to produce thin films of indium tin oxide on a wide range of

substrates. It is one of few techniques suitable for experimental use with polymer substrates as no post-processing is required, and substrate temperature can be easily controlled. The substrate must be securely attached to a heater and loaded into a chamber, which is evacuated to achieve a high level of vacuum. The substrate can then be brought up to temperature in preparation for deposition, and oxygen or other gases may be added to achieve the desired composition. A laser is fired into the chamber via a series of focussing and reflecting lenses, and strikes the indium tin oxide target. The high energy of the laser ablates the target, causing a plume of ionized gas to be ejected from the surface. The plume will then hit the substrate, and deposit a small amount of indium tin oxide on the surface. Once this has cooled, the substrate may be cooled, the vacuum decreased, and the sample is ready(Chrisey and Hubler 1994).

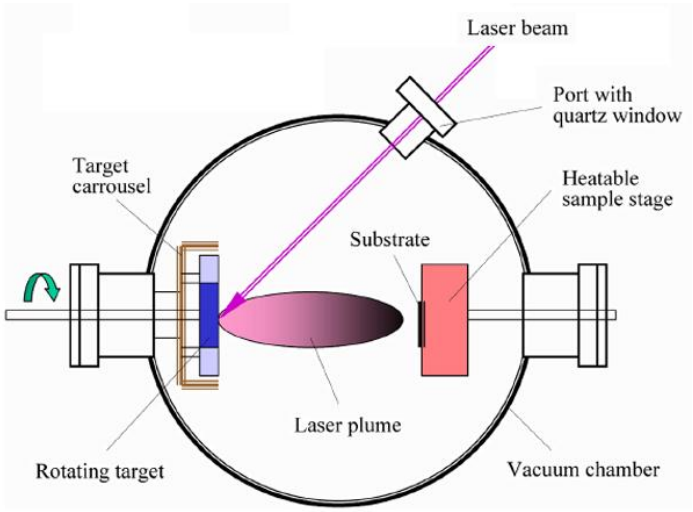

Figure 10. PLD apparatus (Chrisey and Hubler, 1994).

Whilst PLD is a useful method for preparation of individual samples, the relatively small size of the ablated plume means that it is not suitable for the manufacture of large sheets, or mass production – an area of 8 inches diameter, as deposited by Greer and Tabat (Greer and Tabat 1995) is believed to be the largest current demonstration of PLD. According to Eason (Eason 2007), the advantages of PLD over

other comparable process (such as room temp magnetron sputtering), include the ability to produce crystalline films at low temperatures because the ionized particles have very high kinetic energies of above 1 eV, reducing the need for the input of thermal energy to facilitate crystallisation. PLD also has the benefit of producing films with a composition very similar to that of the target, so the production of a stoichiometric thin film is easily achievable. PLD can produce films with an extremely smooth surface, which will aid its corrosion resistance as discussed earlier.

1.9.4 Inducing crystallinity in samples by changing deposition temperature

The crystallinity of the ITO substrate is determined by several factors, including film thickness, substrate crystallinity, substrate temperature (at deposition), and other variables associated with the PLD process and conditions, such as deposition rate. Murakami *et al* (Murakami, Oya *et al.* 2007) have shown that on polymer substrates, the deposition of a CeO_2 prior to ITO deposition can improve ITO crystallinity. CeO_2 is deposited as a crystalline layer, on which the ITO then finds it easier to nucleate crystals. The resulting crystalline ITO has improved scratch resistant properties. A larger number of crystals will reduce resistivity (Salehi 1998) according to Salehi, mainly by electrical conduction being impeded at grain boundaries through scattering. However, crystalline ITO has a higher conductivity than amorphous ITO due to increased ordering. The change from amorphous to crystalline ITO is also associated with an increase in surface roughness (Lee, Lee *et al.* 2009)

Increased crystallinity was achieved by both increasing substrate temperature and reducing deposition rate, and deposition rate was found to have the greater effect on crystallinity. Work by Potoczny at the University of Birmingham (Potoczny 2009) has shown that regardless of deposition temperature, PLD-produced films of 100nm or less do not appear to be able to achieve crystallinity. Substrate temperature is a very important factor in controlling crystallinity, as increasing temperature increases crystallinity. Alternatively, crystallinity may be induced after deposition by thermal processing (Boehme and Charton

2005)(Dong-Sing, Shui-Yang *et al.* 2006).

It has been shown in ITO-PET systems deposited by magnetron sputtering, that the resistivity decreases as deposition temperature increases from room temperature to 70 °C (Lee, Lee *et al.* 2009). This resistivity drop is attributed to an increase in the density of charge carriers. Between 70 and 100 °C there was an increase in resistivity, due to noticeable cracking of the ITO caused by the thermal expansion mismatch between the ITO and PET. XRD analysis shows no crystallinity at room temperature, a very small 400 peak at 50 °C, and another slightly larger peak at 70 °C. This slight increase in crystallinity is explained by the increase in density of charge carriers. Optical transmittance also increases as substrate temperature increases, because increased ordering reduces the scattering of transmitted light. Similar temperature effects are also noted in ZO films, but at much higher temperatures due to the increased crystallisation temperature(Yang and Zeng 2009). It would appear that any crystallinity at all increases conductivity of the sample, and the negative effects caused by impedance at grain boundaries are easily offset. Increased substrate temperatures are therefore desirable to increase conductivity, as long as no cracking is caused by the thermal expansion mismatch. Increased conductivity of the ITO layer is desirable, as thinner layers may be used for equal conductances, and thinner layers will experience lower strains in bending and so allow more flexible screens.

2 Aims and objectives

2.1 Scope of the project

The aim of this project is to investigate the effect of deposition temperature on the response of flexible ITO-polymer systems to acrylic acid. In order to correctly identify the contributing factors of deposition temperature, samples will be produced at varying temperatures and then tested and analysed to show the effects of deposition temperature.

2.2 Sample production

PLD can be used to manufacture different samples under exactly the same deposition conditions, with only substrate temperature varying. Samples may be produced on a range of polymer substrates including PET, PEN and polyimide (PI). Some samples may also be produced using a commercial magnetron sputtering machine, but temperature control is less precise in this instance, with minimum temperatures being so high that only PI is suitable. These samples can then be characterised to find the effects of deposition temperature on their behaviour.

2.3 Sample characterisation

2.3.1 Strain behaviour

It is essential to characterise behaviour under strain as flexible screens will inevitably be subject to this. Samples can be immersed in acid for varying lengths of time prior to characterisation, with un-immersed control samples also tested for comparative purposes. These samples may be subjected to uniaxial tensile loading with simultaneous resistance measurement, showing how the acid affects their conductive properties under strain. These samples can be viewed post-strain using an SEM to assess the differences in cracking, or *in situ* using a camera.

2.3.2 Wear behaviour

The response of ITO-polymer systems to repeated pressure from small hard particles will directly affect their durability in the manufacturing process and in use. AFM nanoscratching can be used to simulate this situation, with samples immersed in a range of acid concentrations prior to testing.

2.3.3 Surface roughness

As surface roughness can affect corrosion susceptibility, AFM will be used to obtain average roughness measurements for all deposition temperatures.

2.3.4 Crystallinity

One of the most fundamental and measurable differences between samples produced at different temperatures is likely to be the level of crystallinity. To quantify this it is possible to use X-ray diffraction (XRD) and transmission electron microscopy (TEM).

Once the samples are characterized via all these different methods, it should be possible to determine the effect of deposition temperature on the mechanical and electrical properties of ITO-polymer systems subjected to corrosive attack.

3 Experimental method

3.1 Sample production

3.1.1 Substrate preparation

To avoid delamination of samples occurring by the cutting of pre-deposited sheets, ITO must be deposited on polymer samples already cut to shape. Dog-bone shapes for tensile testing were therefore cut from the polymer substrate sheets using a high pressure press, and a blade and foam arrangement to ensure consistency in sample dimensions. Substrates used were PET Melinex ST505 and PEN Teonex 175 (DuPont Teijin Films, V.A., U.S.A.).

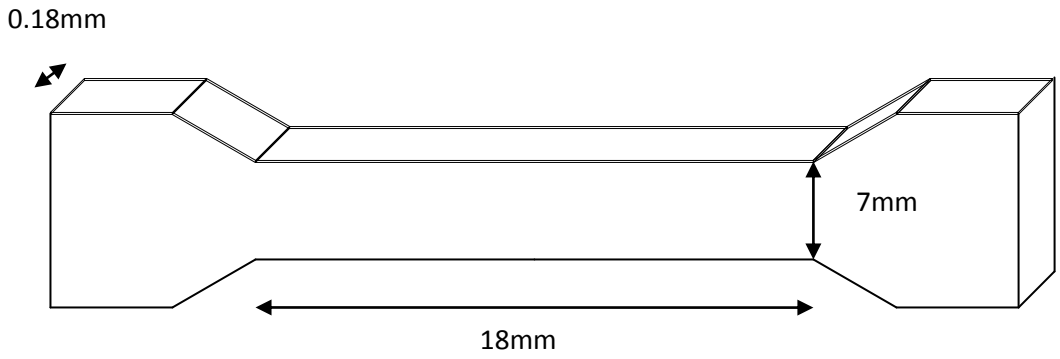

3.1.2 ITO deposition by PLD

Pulsed laser deposition (PLD) was used to deposit ITO on the substrates. The edges of the samples were rubbed with wet and dry paper to remove any burrs or sharpness, and the samples where cleaned ultrasonically in acetone, ethanol and then water. The samples were clamped to a heating stage at either end, ensuring good thermal contact. The sample and heater were loaded into the vacuum chamber, which was evacuated to at least $1x10^{-6}$mTorr. A target-substrate distance of 51mm was used. The samples were heated to their target temperature (50, 100 or 150 °C) at a rate

of 7 °C/min. Oxygen was introduced into the chamber at 7.5mT O_2, to give optimum electrical and optical properties (according to work in the same chamber by Potoczny (Potoczny 2009)). Between 1000 and 2000 laser pulses of 415 mJ were used to deposit, giving a range of thicknesses and film quality. Deposition rate was 10 Hz, and the target was rotated during deposition.

3.1.3 ITO deposition by magnetron sputtering

Samples were also produced using a local commercial magnetron sputtering machine (Diamond Coatings, Birmingham, UK). Dog-bone samples of PI were cut from the uncoated sheet, ultrasonically cleaned, and clamped to an aluminium tooling block (providing thermal mass). This block was then passed under the planar magnetron an equal number of times (unknown, but controlled by the manufacturer to give consistent thickness). Samples were deposited at ambient temperature and at approximately 200°C. A larger range of temperatures was not possible due to the limitations of the heater being used. Samples produced at 200 °C were reheated in a vacuum outside of the sputtering chamber, passed under the magnetron a set number of times, then reheated and resputtered until the required thickness was achieved.

3.2 Sample characterisation

3.2.1 Tensile testing with simultaneous resistance measurement

The conduction behaviour under strain was characterised using an Instron 5566 mechanical testing machine. Nylon bolts were used to attach the bottom clamp to the machine body and plastic sheeting was also placed underneath, ensuring that the samples were electrically isolated. The ITO-coated samples were clamped securely at either end into metal grips, and strained at a constant rate of 0.08mm/min in uniaxial tension. Each clamp is electrically connected to a Fluke multimeter, which can measure the resistance across the sample at a constant current. The strain and resistance data are paired by computer, which can plot them against each other (Labview program). COS can

then be calculated as the strain at which the resistance has increased by 10 %, and the general resistive behaviour of the samples under strain can be observed and analysed. Five COS measurements were taken for each separate deposition and acid immersion condition.

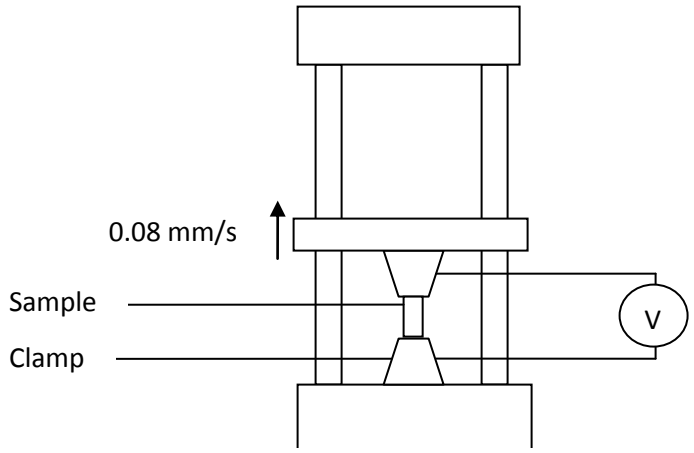

Figure 11 Strain and resistance characterisation equipment

3.2.2 Acid immersion

For each deposition temperature, a minimum of three samples were tested for each corrosion scenario. These were: as deposited (no corrosion); immersed in 0.1M acrylic acid for 30 minutes; immersed in 0.5 M acrylic acid for 30 minutes and immersed in 1M acrylic acid for 30 minutes. Acrylic acid was used as it is likely to come into contact with ITO in device structures for practical applications, as acrylate-based fixatives and glues are commonly used. The acid solution was prepared using 99.8% pure acrylic acid as supplied by Fisher Laboratories mixed with distilled water, in which the sample is fully immersed. There was no agitation or mixing during immersion as the samples are susceptible to damage through bending or collision. Once immersed for the required length of time, samples were then patted dry with a paper towel, and immediately tested in tension to avoid further corrosion.

3.2.3 X-Ray diffraction

Samples were tested for crystallinity using X-ray Diffraction (XRD), for 2θ between 20° and 70°.

3.2.4 SEM analysis

Samples were also observed using a Jeol 6060 Scanning Electron Microscope (SEM) to assess cracking mechanisms, evidence of delamination, crack widths and any other features of interest. Samples viewed in the SEM were gold plated before analysis to improve picture clarity, and images are taken at the middle and the edge of the sample. Images were taken at a range of magnifications. A working distance of 10mm was used, with beam energy of approximately 10eV.

3.2.5 TEM analysis

For analysis of the level of crystallinity, samples were also prepared for transmission electron microscope (TEM) observation. Samples were vertically mounted in a solid resin which was then sliced to give 100nm thick cross-sections of the sample (Figure 12), which were electron transparent. These samples were then viewed in a Phillips 2100 TEM to give images showing crystallites. The TEM was also used to find diffraction patterns of the ITO layer, where any pattern would suggest that some crystallinity had been induced.

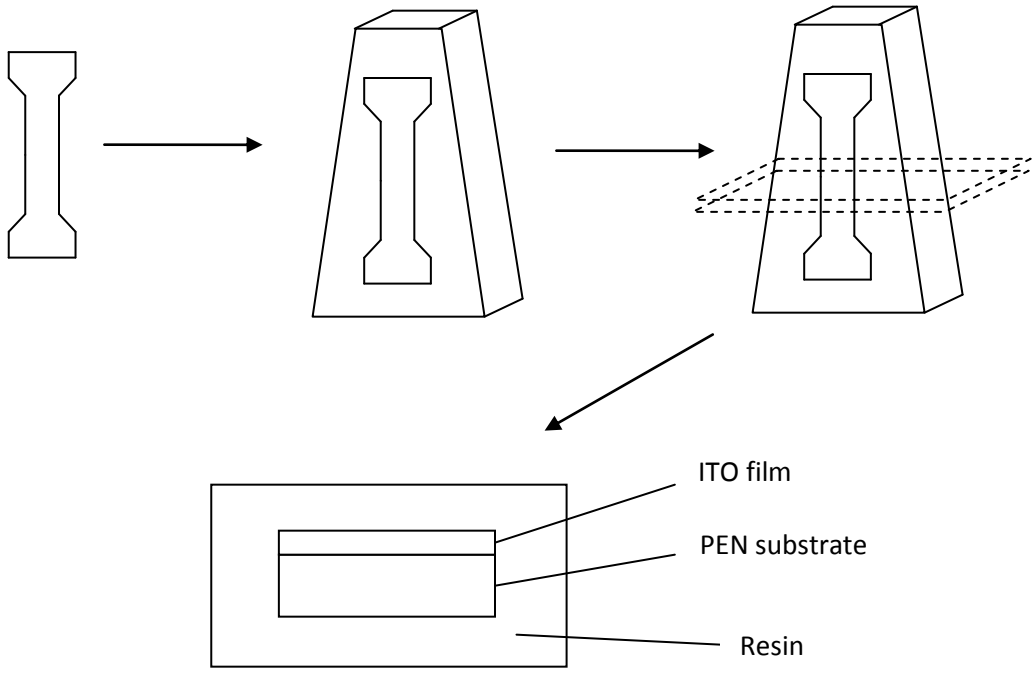

Figure 12 TEM sample preparation process

3.2.6 Atomic force microscopy for surface roughness measurement

Atomic force microscopy (AFM) was used to characterise the surface roughness of samples produced at all temperatures. An AC3100 AFM was used in multidimension tapping mode, with a scan rate of 1.2 Hz. Samples were measured for Amplitude Parameter R_{RMS}(nm) and Profile Roughness Parameter R_a (nm), and the averages of five values taken for each sample.

3.2.7 Fragmentation analysis

Fragmentation analysis was used to show the exact cracking behaviour of different samples. The samples were loaded into a minimat tensile test machine(Biddlestone, Kemmish *et al.* 1986), and were strained in uniaxial tension at a rate of 0.1 mm/min. Resistance was simultaneously measured, and the equipment set up and acid immersion procedures were the same as that previously mentioned. However, microscope with real time video capture was used to observe the sample during this process, giving images of cracks and crack development at specific strains and resistance changes. Images were taken at 3 second intervals.

Two new measurements were found using this technique – Visible Crack Onset Strain (VCOS) and Visible Delamination Onset Strain (VDOS). VCOS is defined as the strain at which cracks perpendicular to the direction of strain are first visually observed in the images taken. VDOS is defined as the strain at which cracks parallel to the direction of strain are first visually observed in the images taken. These measurements are necessarily a matter of judgement on the part of the observer and so there is some margin for error.

VCOS and VDOS were found using the mean value of 3 experimental samples. Measurements were taken for samples immersed in 0.5 and 1 Mol/L acid prior to the application of strain.

3.2.8 Nanoscratching

An AC3100 AFM operating in contact mode was used for the nanoscratching experiments. The diamond coated cantilever used had a spring constant of approximately 0.2 N/m, and a tip radius of approximately 150nm. The tip was loaded into the machine and aligned with the lasers, and the deflection set point then measured on a known hard surface such as stainless steel using the advanced imaging force tool. The force applied per volt could then be found using Equation 1(Bowen 2010):

Equation 1

$$D * C = Fv$$

where D is “Deflection Setpoint” in nm, C is the “Spring Constant” in N/m, and F_v is the “Force Applied per volt” in nN/V.

The sample could then be inserted and the tip engaged. Scratching force could be modified by changing the voltage applied, from a minimum of -8 up to a maximum of 9, giving a maximum voltage increase of 17. Force applied could be calculated using Equation 2(Bowen 2010):

Equation 2

$$Fv * V = Fa$$

where V is the "Voltage increase" in V, and F_a is the "Force Applied" in nN

The surface was initially imaged at 15nN, and then a small area of the image would be subjected to a scratching force of up to 2 µN by changing the voltage applied. This scratching process could then be repeated on the smaller area several times if desired. The original area could then be re-imaged and assessed to see the extent of scratching. Scratch depth and width could be measured and compared between samples using the imaging function of the AFM. Samples produced at different temperatures were characterised in this way, and some samples could be subjected to similar acid immersion regimes to those used in the tensile tests.

4 Results and Discussion

4.1 ITO on PET

To assess suitability for further investigation, six samples of ITO on PET were produced. They were deposited using the PLD conditions described previously, with 2000 pulses and a substrate temperature of 150 °C. One sample was reserved for XRD analysis, one for SEM analysis (Figure 13a), two were tensile tested without immersion in acid (Figure 13b) and two were tensile tested with immersion in acid (1 M, 30 minutes).

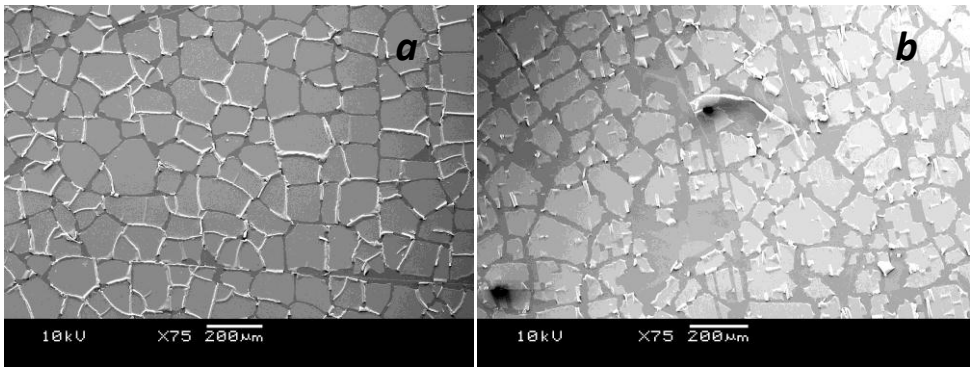

Figure 13. ITO-PET - 2000 pulses, 150°C substrate temp, not tensile tested; and b) ITO-PET - 2000, 150°C pulses, after tensile testing

PET samples are found to show evidence of cracking prior to the application of strain, as Figure 13a shows – at this point no external stress has been applied, but randomly oriented cracks are still visible. Post deposition PET shrinkage would account for this cracking there would be no specific direction of shrink across the sample. From Figure 13b it is also possible to tell that the cracking has occurred prior to the application of strain as the cracking is randomly oriented. Cracking from the application of uniaxial strain typically shows a grid of cracks from cohesive failure at right angles to the direction of strain, linked by cracks from adhesive failure (between substrate and film) parallel to the direction of strain(Morris, Sierros *et al.* 2008).It is also evident that cracking has occurred prior to straining due the initial resistance being recorded for the 2000 pulse/150 °C sample as approximately 7500 Ω (as opposed

to approx 175Ω for the same conditions depositing on PEN – details provided later). The cracking of the film is likely to be due to the larger coefficent of thermal expansion of PET (16 x 10^{-6} °C^{-1} (Ma, Bhushan, 2003)) , in comparison to ITO (7.2 X 10^{-6}°C^{-1}(Wu and Chiou 1997)). There also appears to be poor adhesion between ITO and PET as large sections of the film have fallen off in their entirety, even though the samples have been coated prior to deposition to improve adhesion performance.

These results show that PET is not a suitable substrate for high temperature, pulsed laser deposition of ITO when thicknesses of 200 nm and above are required. Suitability for high temperature deposition is desirable because deposition at higher temperatures increases conductive performance of the ITO. For PET to be used as a substrate in PLD produced films the ITO will either have to be deposited at lower temperatures or with fewer pulses and so a thinner film. Both of these will reduce the extent of cracking and improve the resistance of the component, but the properties of the film would be negatively affected, even assuming no cracking.

4.2 ITO on PEN

28 samples of ITO on PEN were produced. All were deposited using the PLD conditions as described above, with 2000 pulses and a varying substrate deposition temperature. How the samples were used is shown in Table 1. Each sample used for tensile testing was loaded into the Instron machine as described earlier, and strained at a rate of 0.002 mm/min up to 20% strain. One sample from each deposition and acid concentration was used for SEM imaging. Prior to SEM imaging the sample was gold plated.

Table 1.Use of ITO/PEN samples.

	50 C	150 C
SEM	1	1
XRD	1	1
No acid, tensile testing	3	3
0.1 M acid, tensile testing	3	3
0.5 M acid, tensile testing	3	3
1 M acid, tensile testing	3	3

4.2.1 SEM images

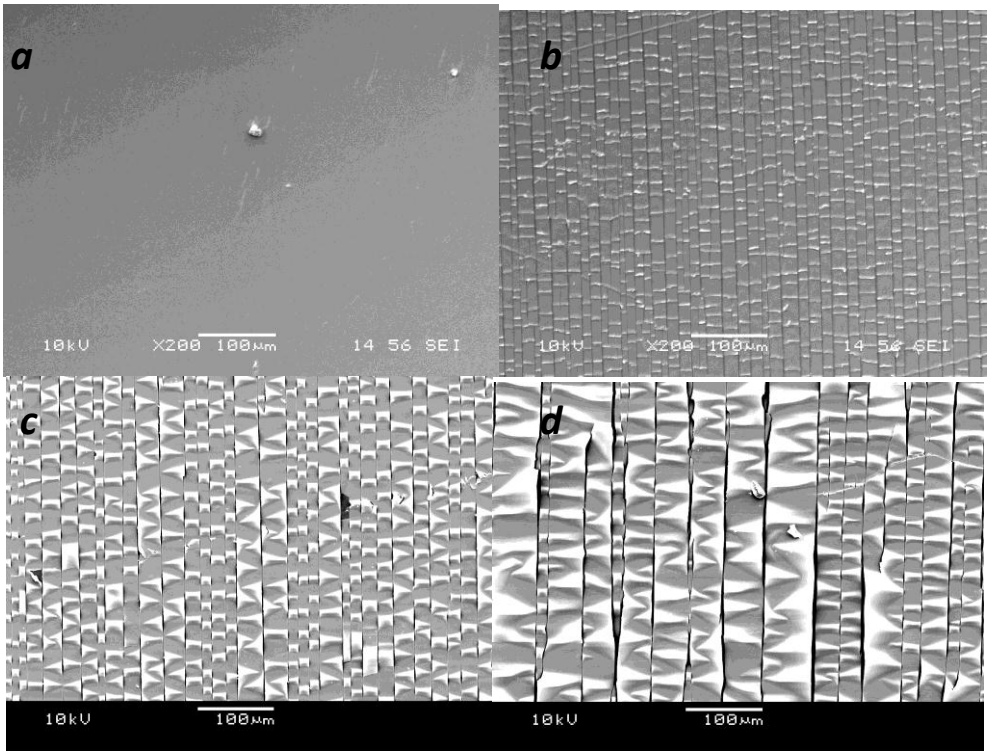

Figure 14 PEN ITO, deposited with 2000 pulses at 150°C. a) As deposited, showing no cracking b) tensile tested, no acid, c) immersed in 0.5M acid and tensile tested, and d) immersed in 1M acid and tensile tested

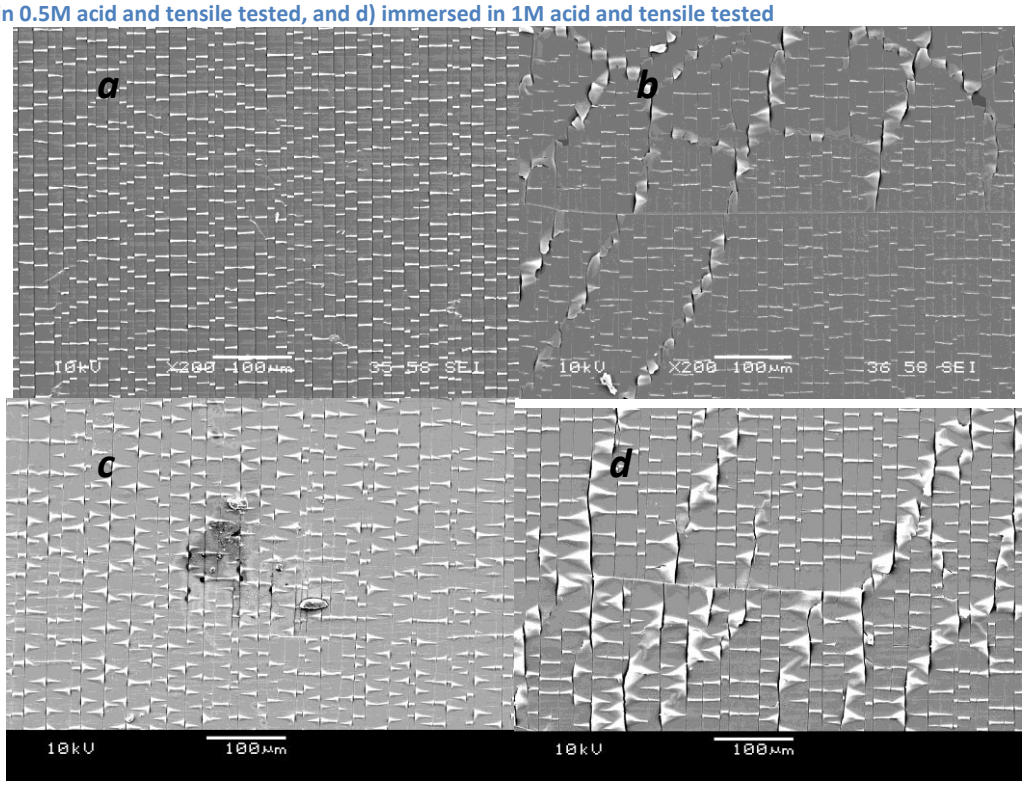

Figure 15 PEN ITO, deposited with 2000 pulses at 50°C. a) tensile tested, no acid b) immersed in 0.1 M acid and tensile tested c) immersed in 0.5M acid and tensile tested, and d) immersed in 1M acid and tensile tested

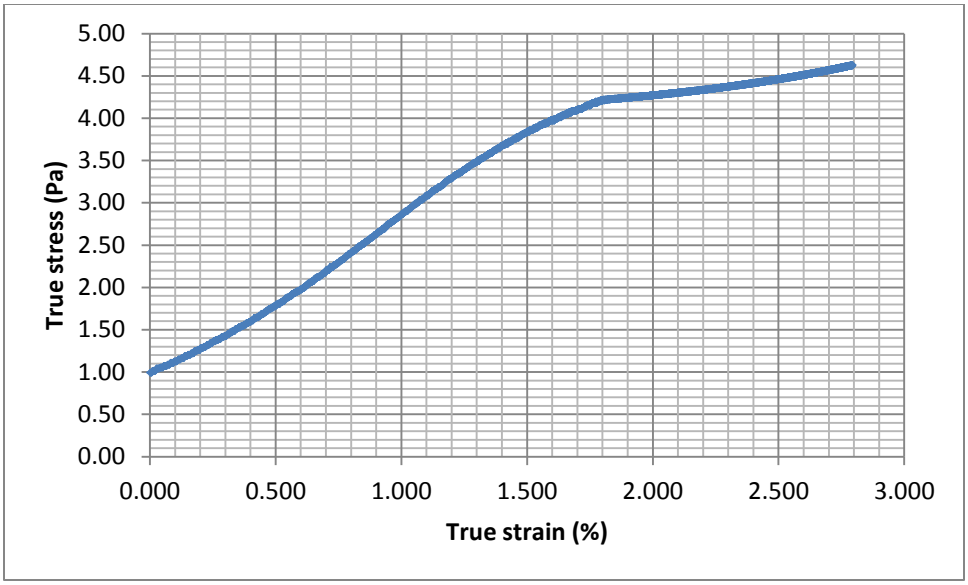

Figure 16 True stress true strain curve for sample deposited at 150 °C and immersed in 1M acid.

In comparison with PET, PEN samples deposited at the same conditions show no cracking before tensile testing (Figure 14a). This indicates that these deposition conditions are compatible with the substrate to provide stable films which are not cracked during manufacture. These samples are suitable for further testing.

Figure 16 shows that ITO on PEN samples behave elastically until approximately 1.8 % strain, after which point they deform plastically. The direction of straining in all samples was from left to right. SEM micrographs show a clear increase in the severity of bridging delamination between transverse cracks as acid concentration increases. The bridging delamination appears to be greater in the 150 °C samples at all concentrations, indicating that adhesion between film and substrate is lower in these samples. Adhesion is known to be strongly affected by thermal mismatch between film and substrate (Wu and Chiou 1997), so this increase in delamination suggests that thermal mismatch is likely to be affecting the failure mechanism. Transverse cracks appear similar in width and frequency across all samples. Particularly in the 50°C samples, there appear to be some longitudinal defects which can act as breaks, stopping transverse cracking. These defects affect the uniformity of the sample and could influence

resistance. These defects are most likely to have arisen from scratches or flaws on the substrate surface prior to deposition, and cracking occurs along them during straining.

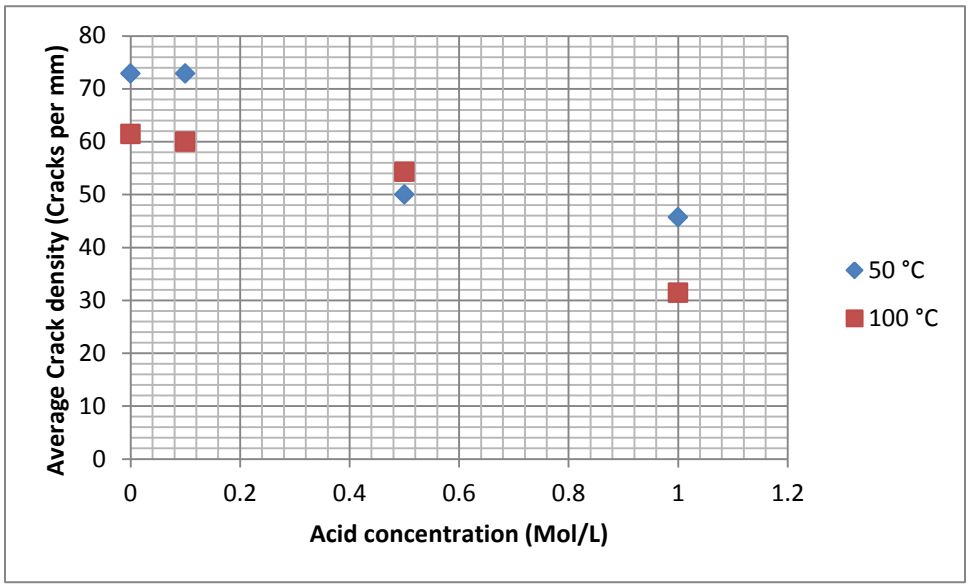

Figure 17 Average crack density for samples produced at 50 °C and 150 °C.

Figure 17 clearly shows that as acid concentration increases, crack density decreases. As it is known that immersion in acid is detrimental to the properties of the ITO film, it may be inferred that weaker films have a lower crack density.

Cracking appears to be less uniform in the 50 °C samples. There are a larger number of types of defect, with the standard cracks being accompanied by singular defects which do not fit the pattern, as in the centre of Figure 15c.

The uniformity of the cracks is very defined and ordered, for which there are two possible explanations. One explanation is that the uniaxial nature of the loading causes very even distribution of stresses, so the cracks will be straight and evenly spaced. This explanation relies on the film and substrates being free from defects and homogenous along their length. Alternatively, the uniformity may arise due to

crystallinity in the ITO film, with the cracks occurring along crystalline planes. If the crystalline explanation holds, we would expect more uniformity of cracking in the 150 °C samples, as these would be more crystalline. We would expect a very low uniformity in the 50 °C samples, as these are expected to have no crystallinity. The crystalline explanation is supported to a point as uniformity is clearly greater in the 150 °C samples, but the 50 °C samples are very uniform anyway. The increased uniformity in the 150 °C samples may be due to increased homogenity in the film as the high temperature improves mobility and makes the film more even, without necessarily inducing crystallinity. The discovery of any evidence of crystallinity in either of the samples will help to determine which explanation is most likely.

4.2.2 ITO on PEN resistance data

During tensile testing the resistance of each sample was continuously monitored. The average resistance and COS are calculated to two decimal places using the mean of the three samples tested. The error given is the standard deviation of the three samples.

Table 2. Average initial resistance and COS data for different samples immersed in acid for varying lengths of time.

Substrate	Deposition temperature (±2 °C)	Acid (±0.01 M l^{-1})	Average Initial Resistance (Ω to 2 d.p.)	Average COS (% to 2 d.p.)
PET	100	No acid	418.90	1.34
PET	150	No acid	7446.82	0.49
PEN	50	No acid	250.03	2.25
PEN	50	0.1	237.86	2.13
PEN	50	0.5	219.92	1.66
PEN	50	1	226.04	1.84
PEN	150	No acid	180.07	2.63
PEN	150	0.1	175.38	2.37
PEN	150	0.5	179.16	1.80
PEN	150	1	226.95	1.37

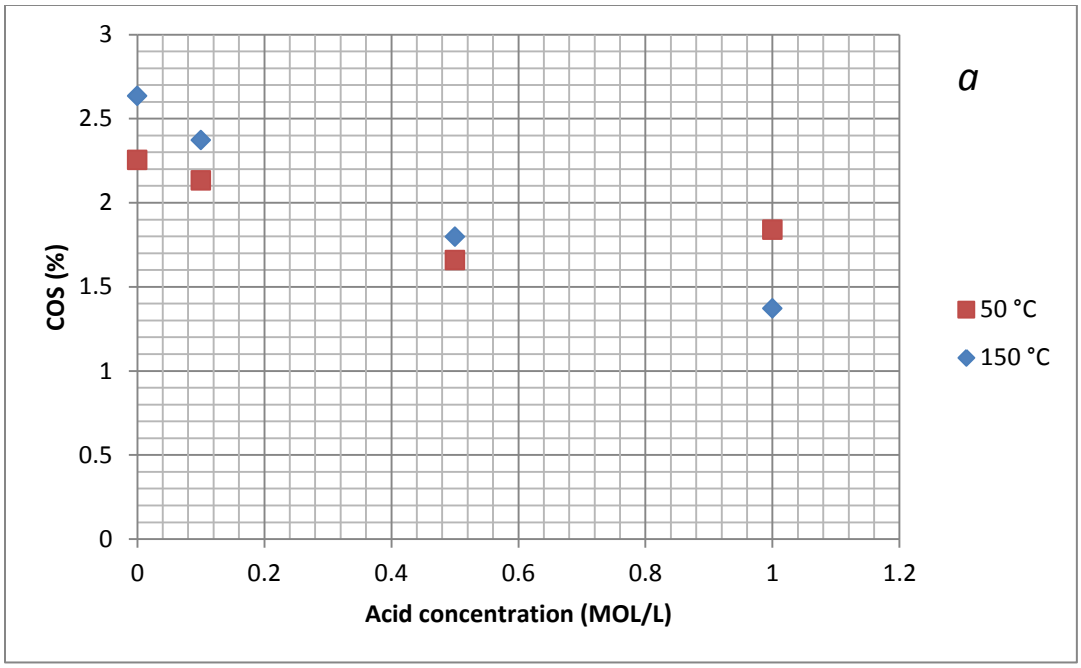

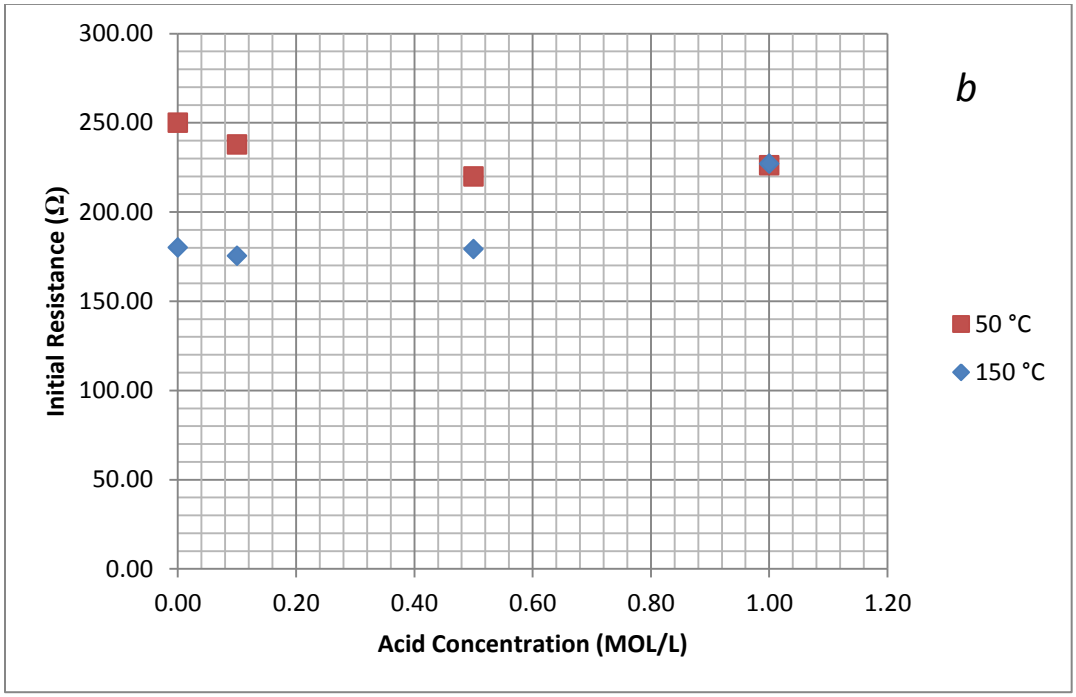

Figure 18 Average values for COS (a) and initial resistance (b) against acid concentration.

For each deposition temperature and acid immersion condition a resistance profile is shown in Figure 19.

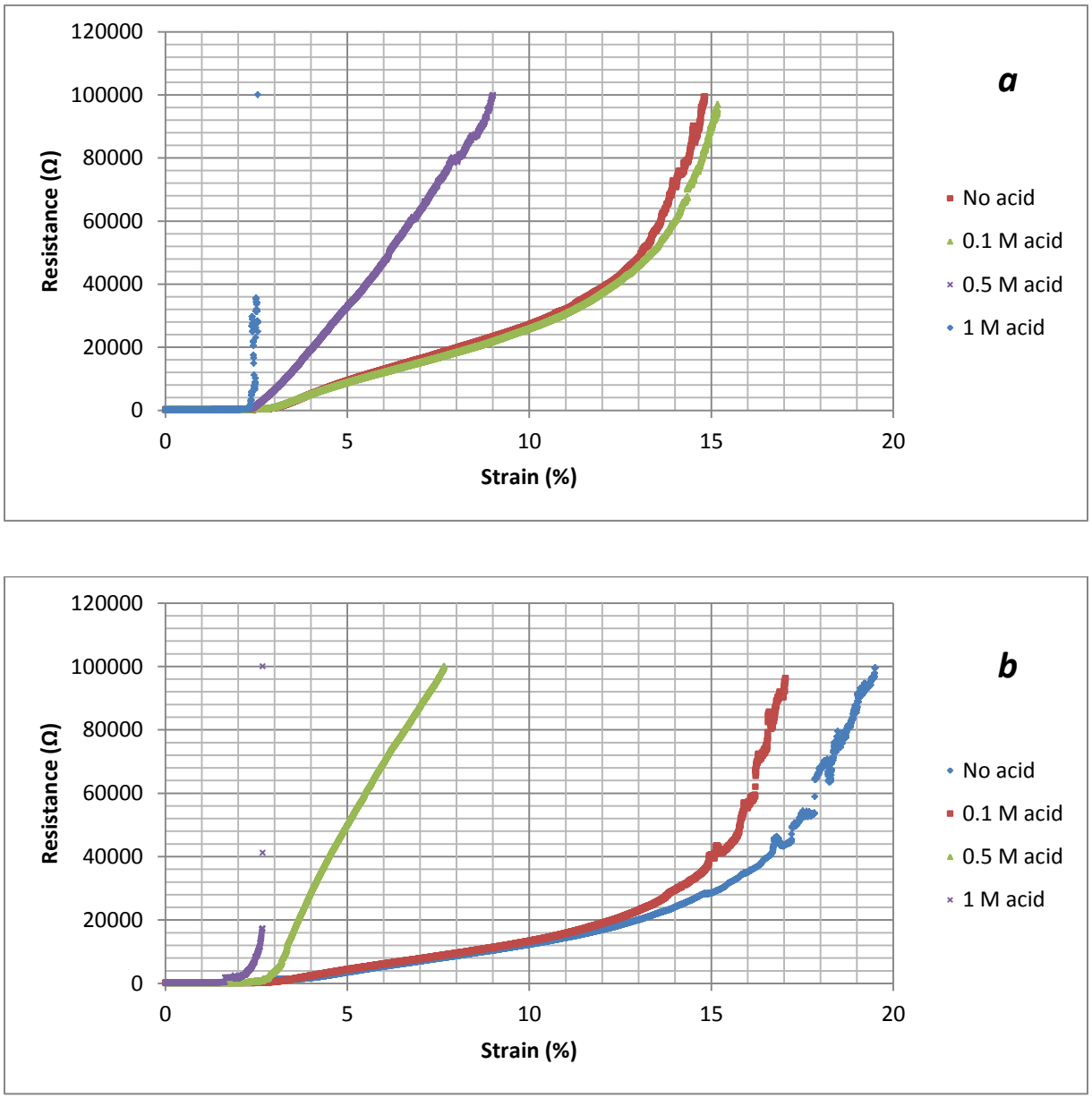

Figure 19 Resistance plotted against percentage strain for samples deposited at a) 50 °C and b) 150 °C

Figure 18a indicates that samples deposited at either deposition temperature show a decrease in COS as acid concentration increases. This supports work by Morris, Sierros *et al.* (2008) which shows that increasing acid concentration decreases the ability of a sample to resist strain. Figure 17 clearly demonstrates that increasing acid concentration decreases crack density, so it is evident that decreased COS cannot be due to increased crack density – earlier crack initiation is therefore a more likely candidate. The exact mechanism of corrosion is unknown, but the acid is thought to attack the indium-oxygen bonds, weakening the film. The corrosion mechanism cannot simply be a uniform thinning of the ITO layer across the whole surface, as thinner as-deposited layers have higher COSs. The corrosive attack could therefore be non-uniform and focussed on preferential sites, causing weak points on the film which are more likely to crack.

Samples deposited at 150°C show a sharper decline in COS as acid concentration increases, suggesting that they are more affected by the presence of acid. One explanation of this could be the increased temperature-induced crystallinity, with the grain boundaries acting as preferential sites for corrosion (Folcher, Cachet *et al.* 1997). Alternatively, the increased temperature could be responsible for larger stresses between the film and substrate, due to a mismatch in thermal expansion during deposition and subsequent cooling. The increased stresses on the film could make it more susceptible to corrosive attack, whilst the samples deposited at 50 ℃ have a lower residual stress and are not as susceptible to corrosive attack. Figure 18b supports Figure 18a in showing that samples deposited at 150 °C are more sensitive than samples deposited at 50 °C to an increase in acidic concentration.

Figure 19 shows the effect of acid concentration on the resistance increase during tensile loading up to very high strain and resistance values. Whilst the changes in COS and initial resistance between different acid concentrations are very small, the behaviour post-COS is markedly different. Behaviour post-COS is not of as much interest in terms of suitability for touch screen applications, as we are trying to avoid

cracking altogether in that system, but it is nevertheless interesting as the difference is so severe and noticeable. It is also worth investigating for applications which may require only low levels of conductivity, where cracking is acceptable and possibly expected.

Samples that were not immersed in acid show a very gradual increase which continues to strains beyond 20%. Samples that were immersed in stronger acidic solution increase gradually up to strains of approximately 2 – 2.5 %, before a more rapid increase in resistance is observed, and total resistive failure soon follows. This increase is sharpest for samples immersed in 1 M acidic solution. This behaviour is analogous to that shown by (Morris, Sierros *et al.* 2008)where increasing acidic concentration decreased the time it took for samples to fail, both under the application of load and in static situations.

Samples deposited at 150°C appear to increase in resistance more gradually than those deposited at 50°C for non-immersed samples, eventually reaching 100 kΩ at higher strains. The samples also have a lower initial resistance and a higher COS, so their conductive performance is better in every aspect, assuming no acid is introduced. This enhanced performance at high strains lends more weight to the crystallinity explanation for the acid effect on COS caused by increased deposition temperature, as we would expect the residual stresses in the 150 C samples to be affected by increasing stress also if thermally-induced stresses were the cause.

It is clear from Figure 19 that deposition temperature does have some impact on the post-COS behaviour of the sample, but ultimately the general trend follows the same pattern for each acid concentration regardless of deposition temperature. The SEM images from fig 14 indicate that earlier stages of cracking are concerned with cohesive failure, and the later stages concern adhesive failure. In some substrate/film systems (Wei and Chen 2008), thermal mismatch is shown to primarily affect adhesive behaviour, so if thermal mismatch was causing differences between the samples, we would

expect the samples deposited at a high temperature to behave differently in the later stages of the graph. The SEM images in fig 3 show us that adhesion is lower in the 150 °C samples, so whilst adhesive failure may be occurring due to thermal mismatches, it happens at the later stages of the cracking process and does not affect the resistive behaviour of the sample to a significant extent.

4.2.3 Fragmentation analysis

Acid concentration (Mol/L)	Mean VCOS (%)	Mean COS	Mean VDOS (%)
0.5	3.31	3.11	7.91
1	3.32	3.11	8.28

Table 3. Mean VCOS, COS and VDOS to 2 d.p. of fragmentation analysis samples immersed in 0.5 and 1 Mol/L acid concentrations. 3 samples were tested at each concentration and then used to calculate the mean.

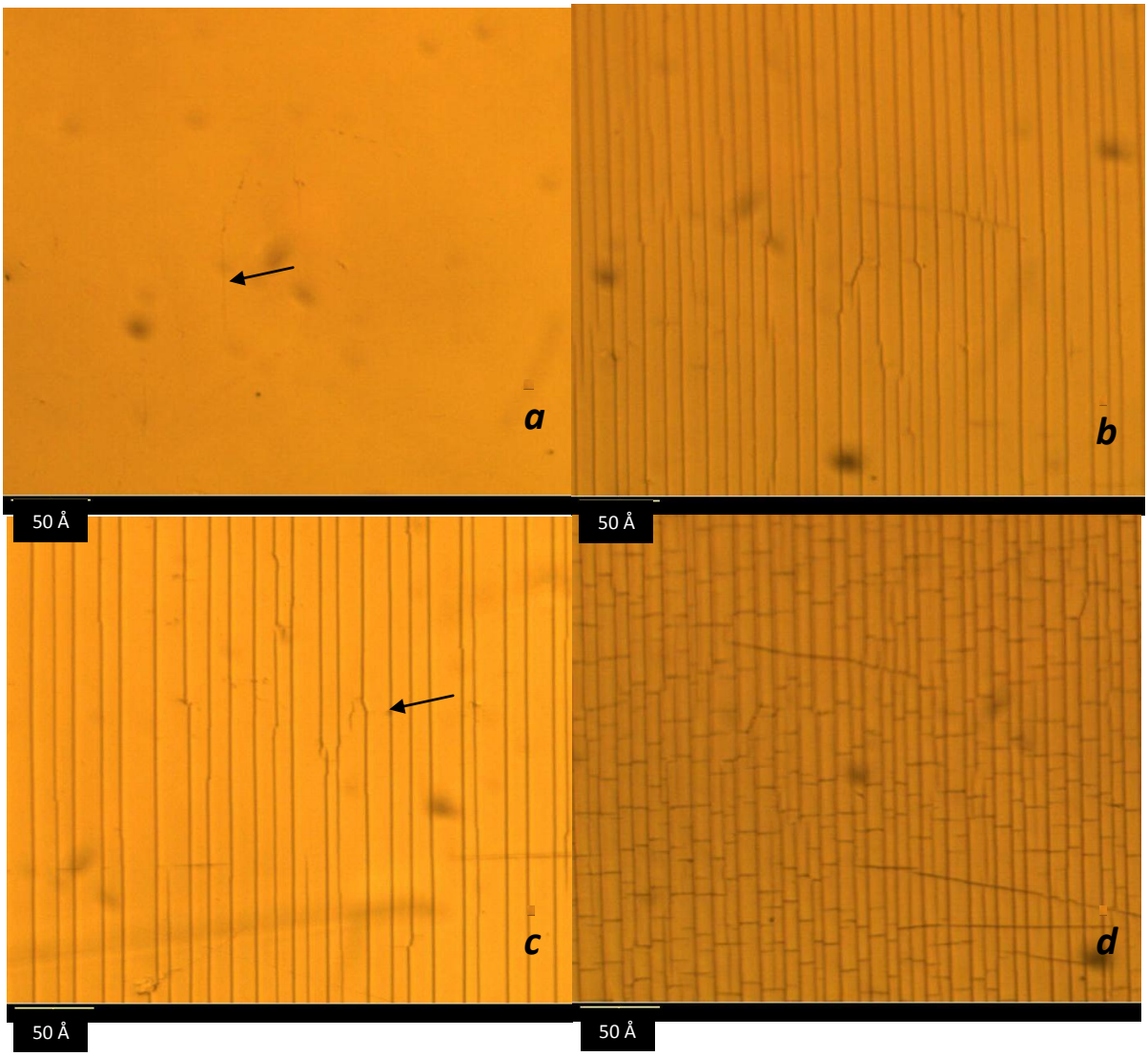

Figure 20. Sample immersed in 0.5 Mol/L acid. Images taken at a) 3.11% strain, as the first vertical cracks appeared; b) 5% strain; c) 8.39% strain, as the first horizontal cracks appeared; d) 11% strain. Arrows denote the location of the first horizontal (a) or vertical (c) cracks.

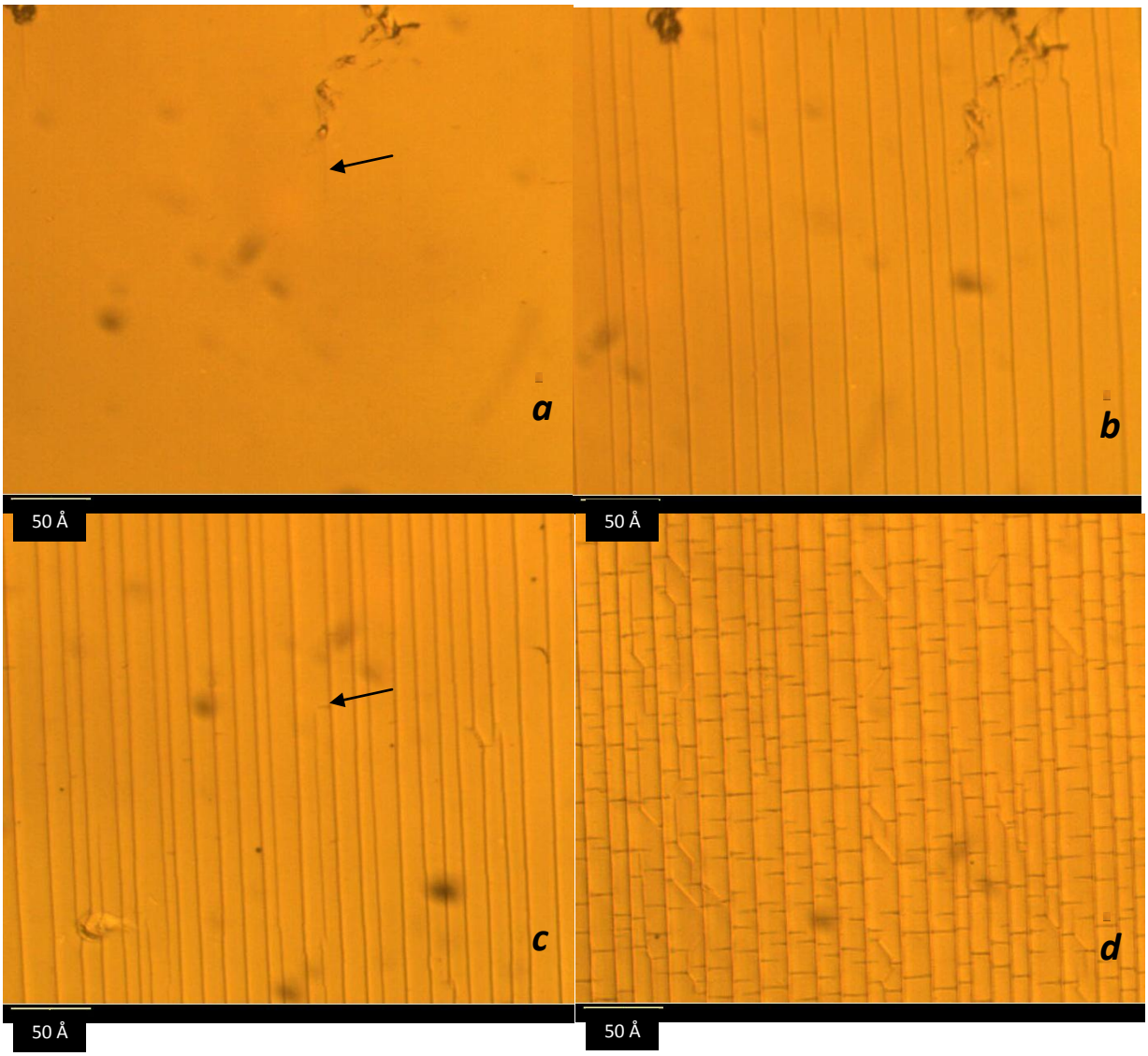

Figure 21. Sample immersed in 1 Mol/L acid. Images taken at a) 3.06 % strain, as the first vertical cracks appeared; b) 5% strain; c) 8.11% strain, as the first horizontal cracks appeared; d) 11% strain. Arrows denote the location of the first horizontal (a) or vertical (c) cracks.

Figure 20 and Figure 21 show that the cracking behaviour of samples immersed in acid concentrations between 0.5 and 1 Mol/L is almost identical. Table 3 demonstrates that visible vertical cracks appear at very similar strains in both samples. Visible horizontal cracks appear later in samples immersed in higher

acid concentrations, contradicting results from Figure 19 which suggest that immersion in a higher concentration of acid will decrease performance at higher strains.

Interestingly, the VCOS is higher than the calculated COS by a uniform amount across all samples, indicating that the actual crack onset strain would be closer to 12 % strain than the 10 % used as standard. Alternatively, cracks may begin at 10 %, corresponding to the standard calculated COS but at a size which is undetectable by the equipment used in this study. In either instance the COS remains a useful measurement as a means of comparing different samples – whether it indicates the exact moment at which a crack appears is not strictly essential.

Figure 20. Sample immersed in 0.5 Mol/L acid. Images taken at a) 3.11% strain, as the first vertical cracks appeared; b) 5% strain; c) 8.39% strain, as the first horizontal cracks appeared; d) 11% strain. Arrows denote the location of the first horizontal (a) or vertical (c) cracks. Figure 20 and Figure 21 also confirm the supposition that vertical cracks appear and grow first, and horizontal cracks appear only once vertical crack saturation has been reached.

4.2.4 XRD data

XRD data has shown so far that no samples contain any crystallinity in the ITO. XRD traces show only one peak, and this peak can be attributed to the crystalline regions in the semi-crystalline polymers used. ITO layers are only 200nm thick, so the substrate will contribute to the XRD trace. The peak which would be expected from crystalline ITO does not appear, and previous studies suggest that we may expect crystallinity in ITO films produced at 150 °C. It is unclear whether the lack of an ITO crystalline peak is due to a totally amorphous structure in the ITO, or because any crystallinity in the film is not detected by the XRD equipment. Tarey, Rastogi and Chopra (1987) explain how the θ-2θ technique, as used in this experiment is not particularly useful for thin films due to poor sensitivity and substrate effects. Therefore TEM will be used to detect crystallinity as it has a much higher resolution. By using TEM we can remove the substrate effects and detect low levels of crystallinity that the XRD may not be able to pick up.

4.2.5AFM surface roughness

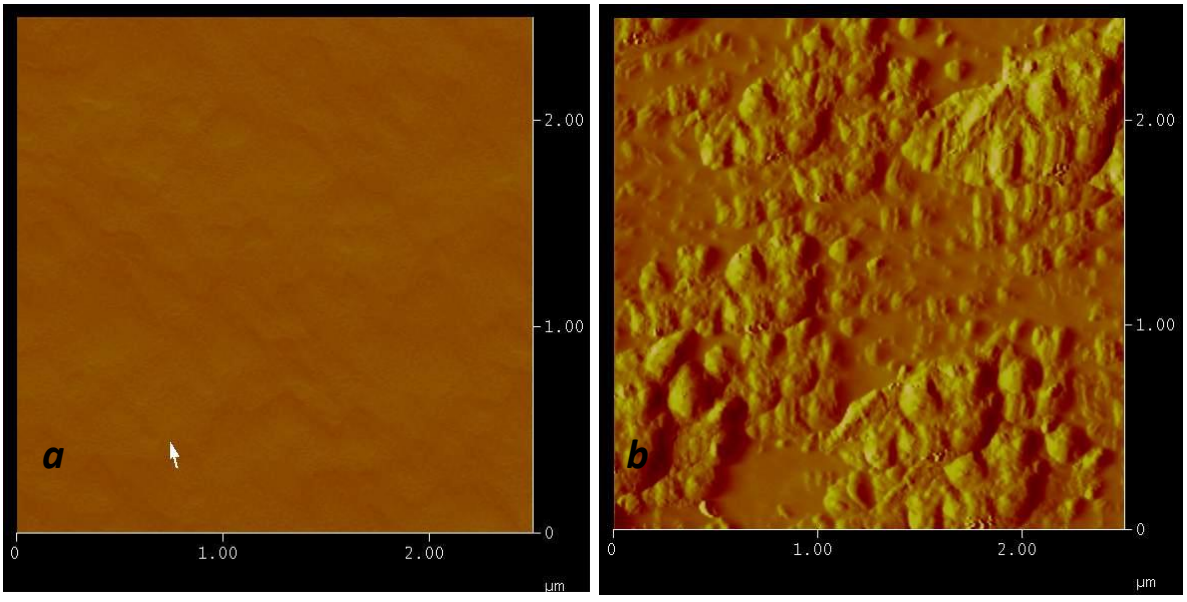

Figure 22 AFM surface roughness images for samples deposited at a) 50 °C and b) 150 °C

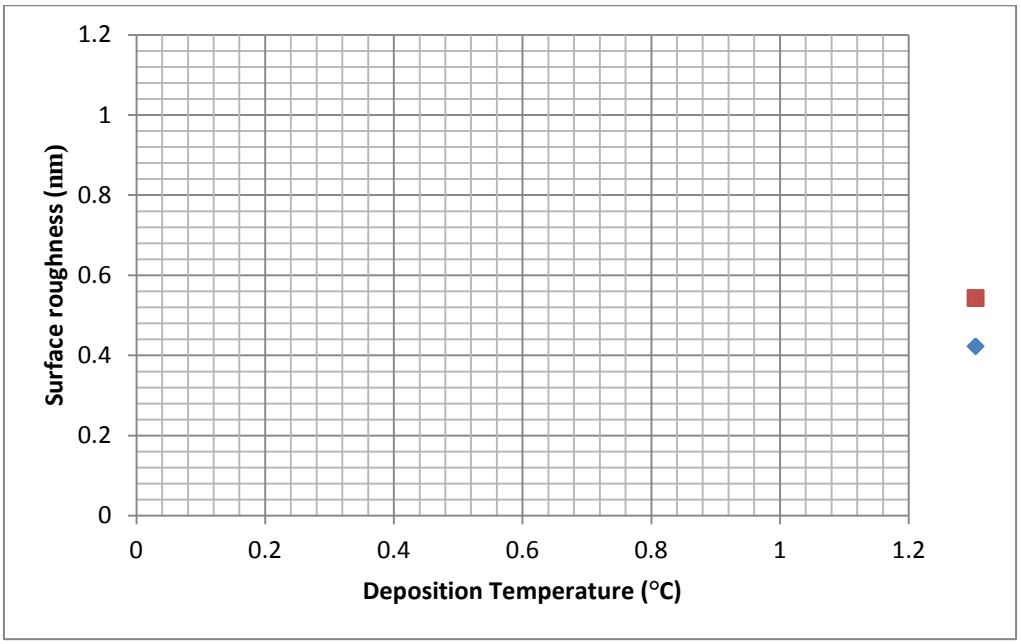

Figure 23. AFM Surface roughness measurements (2.5 nm scale) of samples deposited at 50, 100 and 150 °C

It is clear from Figure 22 and Figure 23 that there is a large increase in surface roughness as deposition temperature increases. Figure 23 indicates that the sharpest rise comes between 100 and 150 °C. Work by Lee *et al.* (2009) has linked the introduction of crystallinity to an increase in surface roughness as crystals grow preferentially, appearing as islands protruding above the level of the non-crystalline material – as can be seen in Figure 22. This increase in surface roughness, and the high temperature required for it, shows that samples produced at 150 °C should therefore contain crystallites. As well as providing evidence of crystallinity, the increase in surface roughness may also provide an alternative explanation for the increased sensitivity to corrosion of samples produced at a higher temperature. The increased surface roughness increases the overall surface area of the film, increasing the area on which corrosion may take place.

4.2.6 TEM analysis for crystallinity

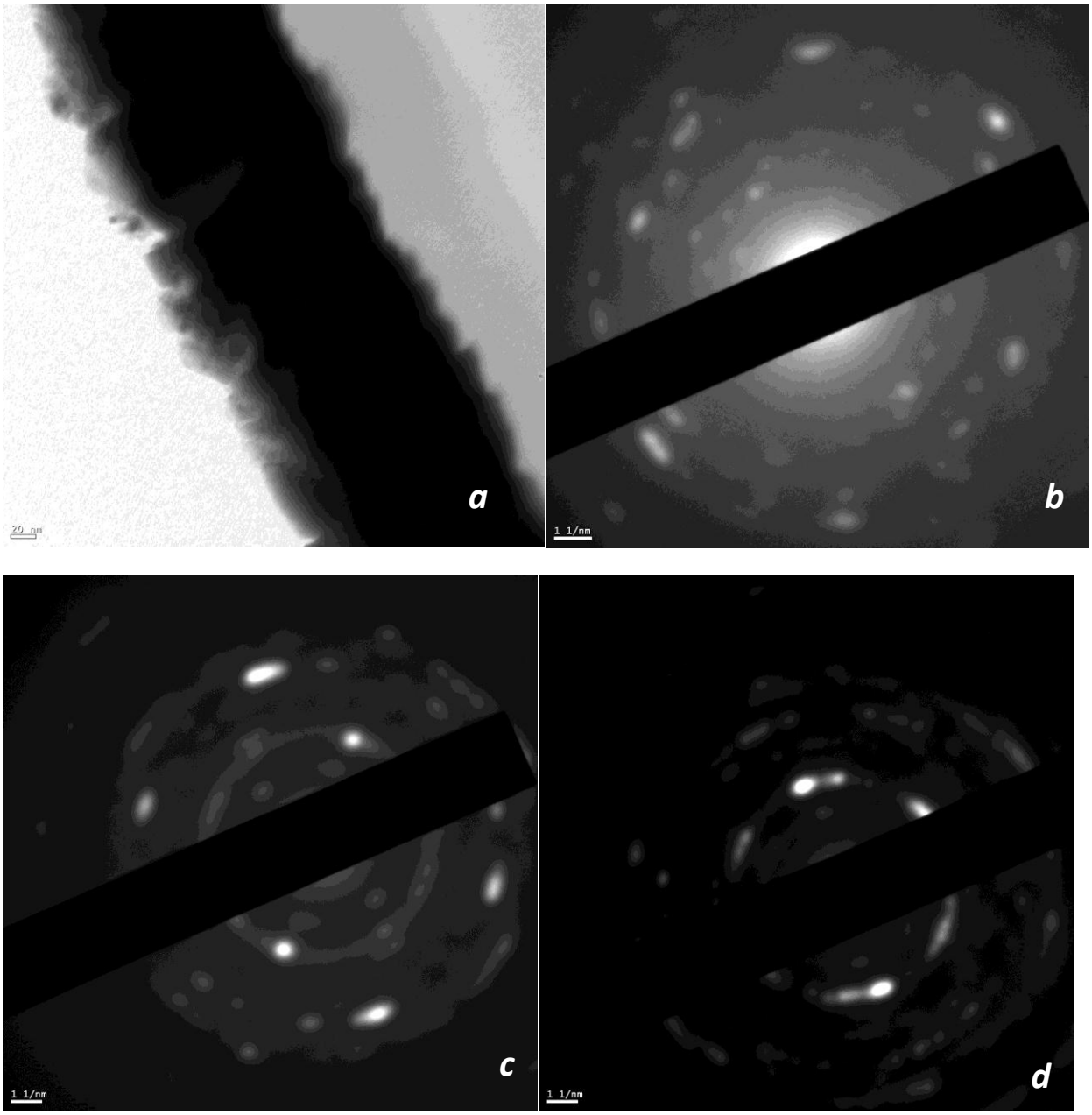

Figure 24 a) TEM image of an example of the cross section analysed. The black strip in the middle is the ITO film and the grey area to the right is the PEN. The Diffraction patterns in a, b and c were taken in the centre of the ITO strip. Diffraction patterns of the ITO are shown for sample deposited at a) 50 °C, b) 100 °C and d) 150 °C.

Figure 24 a/b/c clearly shows that each sample contains crystalline ITO as diffraction patterns only appear when there is crystalline material present. This is surprising as samples at 50 °C were expected to be fully amorphous, with crystals expected to form in the ITO only at higher deposition temperatures, as supported by Figure 23. Figure 24 appears to disprove this hypothesis, although from these images it is not possible to determine the ratio of crystalline to amorphous material, or the size of the crystals present. While crystalline material is present at all deposition temperatures, the increase in surface roughness in Figure 23 could be attributed to an increase in size of the grains grown due to the increased temperature.

4.3 Commercial Samples

Table 4 Average values for initial resistance and COS for PI samples with and without acid immersion

Substrate	Deposition temperature (°C)	Acid strength (Mol/L)	Initial Resistance (Ω)	COS (%)
PI	~200	0	60.74	0.49
PI	~200	0.5	68.97	0.12

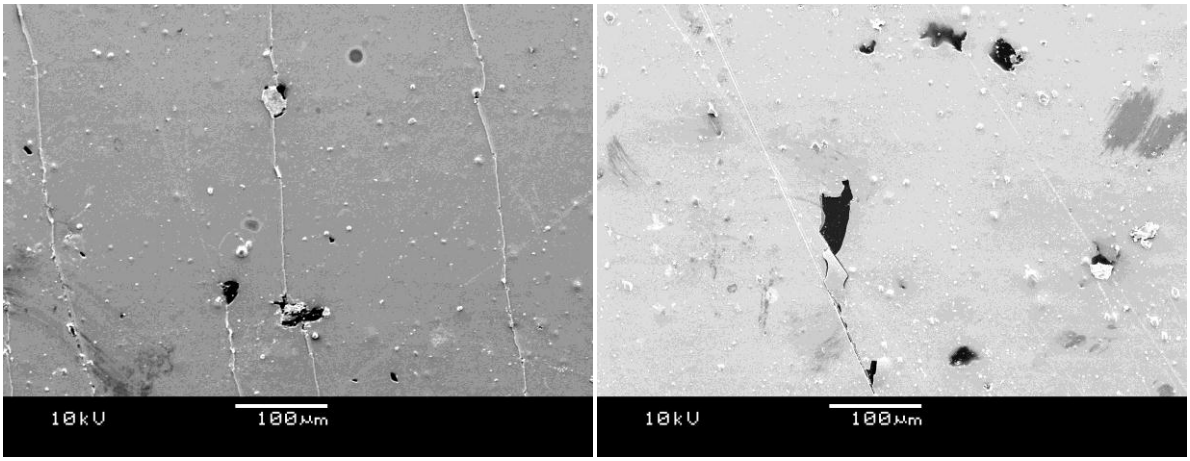

Figure 25 Commercially sputtered PI, deposited at approximately 200 °C. a) Not immersed, tensile tested and b) immersed in 0.5 M acid and tensile tested.

Table 3 shows that the commercially sputtered samples experience a marked decrease in COS after the samples have been immersed in the acidic solution. However, this COS value is considerably lower than the COS values found for PLD produced PEN samples (between 1.3 and 2.8%, as shown in table 2), showing that the failure mechanisms are likely to be remarkably different.

Calculations using resistivity and sheet resistance data provided by the manufacturer, for the commercially produced PI samples, show them to have a thickness of approximately 700 nm, as opposed to the 200nm thickness of PLD samples. This data was not further investigated because each

sample had curled over itself many times, which was likely to cause cracking on such thick films. From the samples tested there was a very high range of initial resistances and COS values, indicating that the samples were not consistent enough for a detailed investigation of intrinsic properties. Also, analysis of load – strain curves indicated that the samples slipped in the clamps by a considerable amount.

SEM micrographs in Figure 25 show that tensile testing does not produce a relatively uniform network of transverse cracks across the length of the sample bridged by secondary cracks, but rather one catastrophic crack is observed in each sample regardless of acid concentration. These catastrophic cracks extend across the width of the sample via a non-linear route, and are assumed to be the cause of resistive failure. Delamination is limited to several small patches of ITO totally detaching from the substrate. In general these patches are located along the catastrophic crack. This indicates that adhesion is reasonably high on the sample and delamination will only occur after cracking, growing on initiation sites along the crack. This high adhesion is most likely due to the high temperature stability of the polyimide causing a lower mismatch in coefficients of thermal expansion. This may also have been helped by the addition of a thin silicon buffer layer between the ITO and the PI. Considering that the ITO was deposited at approximately 200 °C, the high adhesive strength of these samples is very impressive.

4.4 Nanoscratching

The nanoscratching program described in section 3.2.8 was used, with a diamond tip, to characterise ITO on PEN samples. The force applied was gradually increased from 15 nN up to a maximum achievable force of 440 nN. Even with 20 passes over the same area the ITO could not be scratched. Two reasons were proposed as to why no scratching was observed. It could have been due to substrate deformation caused by the soft PEN, a factor which is known to affect many wear experiments on hard films on soft substrates. Alternatively, it may have been that the force applied was not strong enough to scratch the ITO, and that a stiffer cantilever would be required to cause scratching for this material.

In order to establish what caused the lack of scratching, a sample of ITO deposited on glass was also obtained. As glass is a hard material, there should be no substrate effects in this case. Once again, no scratching was observed, so it can be confirmed that the soft substrate was not the only cause of the PEN sample not being scratched. A silicon nitride tip was then used instead of the diamond tip, as it had a higher spring constant and so the ability to exert more force. This tip was used to achieve a scratching force of 3 µN, and still no scratching was observed even after 20 passes over the surface. It can be inferred from this data that ITO is a very hard material and would need a force of greater than 3 µN to scratch it. Substrate deformation may play a role in nanoscratching of ITO on PEN substrates, but it is impossible to tell. As it was not possible to begin scratching on ITO, no tests were conducted on different temperature samples or prior to acid immersion, so it is impossible to tell whether these influence the behaviour.

5 Conclusions

5.1 Conclusions

- When deposited via PLD at a thickness of 200 nm and a substrate temperature of 150 °C, ITO on PET will crack due to thermal mismatch, and would be unsuitable for applications requiring electrical conductivity. ITO deposited on PEN at the same conditions has a lower thermal mismatch and does not crack or break, making it a more suitable candidate for conductive applications.
- 200nm thick films of ITO on a PEN substrate deposited via PLD with a substrate temperature between 50 °C and 150 °C will contain some degree of crystallinity, as shown by TEM diffraction patterns. Between 100 °C and 150 °C the increased temperature causes a significant increase in surface roughness, indicating increased grain size.
- It is unknown whether the uniformity in the cracking is due to cracks occurring along crystalline planes as no amorphous samples have been produced for comparison.
- If a sample is immersed in acrylic acid prior to the application of tensile strain, increasing the concentration of the acid reduces the sample's crack onset strain. This is due to weakening of the ITO film from corrosion.
- Samples deposited at a higher temperature are more sensitive to an increased acid concentration. At higher temperature there will be increased residual stresses (due to thermal mismatch) weakening the film and increased surface area for the corrosive attack, but also potentially increased grain size providing fewer grain boundaries for preferential corrosive attack. As the COS for samples produced at 150 °C decreases much faster with increasing acid concentration than that of samples produced at 50 °C then the effects thermal mismatch and increased surface area must dominate conductive behaviour compared with the reduction in corrosive attack from fewer grain boundaries.

- Increasing deposition temperature decreases the rate at which conductivity drops as strain increases after the COS has been exceeded. Adhesive cracking is the main failure mechanism in this stage, and higher temperature deposition normally decreases adhesive strength, so there must be an alternative mechanism countering this. This mechanism is unknown.
- Cohesive cracks perpendicular to the direction of strain are the first to form and dominate the pre-COS failure of the sample. Adhesive cracks form after COS has been surpassed.
- Commercially produced magnetron sputtered samples fail via one single catastrophic crack and are not analogous to PLD produced samples.
- Using nanoscratching techniques more than 3 μm of force will be required to scratch 200 nm thick PLD produced samples.

5.2 Future work

Initially it is important to fully confirm the conclusions of this thesis. To this end, samples should be deposited at 75, 100 and 125 °C and characterised and tested according to the methods already used. This would give more data and so confirm the accuracy of all trends which have been noted.

Another useful addition would be the testing of different thicknesses of ITO. In this investigation, all samples were deposited with 2000 pulses, giving them a thickness of 200nm. This thickness directly affects the cracking and failure mechanism of the samples, with thicker samples having a lower COS, and thinner samples being much more flexible. Therefore, it is important that many different thicknesses are tested to see whether the conclusions found in this investigation are applicable to all thicknesses of ITO, or just the system tested.

Different substrates should be investigated, as this would affect the adhesive properties of the sample and so change the cracking mechanism.

It would also be helpful to explore different deposition methods, to assess whether the conclusions found are only applicable to Pulsed Laser Deposition. Magnetron sputtering should be investigated as the currently favoured commercial method of ITO deposition. For this an experimental machine would be required with fine temperature controls, rather than the crude commercial set up which was briefly explored in this thesis.

It is also clear from this work that the inducement of crystallinity in ITO on plastic is not fully understood, and often hard to predict. A systematic investigation into the percentage crystallinity of samples produced at different temperatures would aid the understanding of ITO-polymer systems and improve production methods and conditions for use in device structures. It would also be valuable to change ITO thickness and measure percentage crystallinity, as thickness also affects how easily crystals can nucleate and grow.

Wear properties of ITO have been touched on in this thesis, and they will be very important for manufacturing conditions in the large scale production and use of flexible displays and touchscreens. Little is known about the wear properties of ITO on polymers as the softness of the substrate means that ITO characterisation is difficult. As the nanoscratching experiments were not successful, stiffer cantilevers should be used in order to achieve the successful nanoscratching of ITO on polymers. Alternatively a nanoscratch tester could be used, as described by Sierros et al (2011) applying loads in the mN range.

Due to the substrate softness issues, it would be sensible to investigate the systems themselves, as opposed to attempting to determine intrinsic ITO properties. This could be approached by producing samples of ITO (perhaps of different thicknesses) on a variety of different substrates and then subjecting them to a simulation of the wear expected in use (For example, repeated application of stylus/finger pressure), with simultaneous resistance measurement. Post wear microscopy could then be conducting,

showing how the different samples failed. The results could be compared and a “best system” found, but it would be difficult to draw any intrinsic properties out of this.

References

Aleksander, M. and S. J. Klosowicz (2004). Possibilities of application of polymer-dispersed liquid crystals in information displays, USA, SPIE-Int. Soc. Opt. Eng.

Allan, R. (2006). "E-paper chase nears the finish line." Electronic Design**54**(13): 47-55.

Anguita, J. V., M. Thwaites, *et al.* (2007). "Room temperature growth of indium-tin oxide on organic flexible polymer substrates using a new reactive-sputter deposition technology." Plasma Processes and Polymers**4**(1): 48-52.

Biddlestone, F., D. J. Kemmish, *et al.* (1986). "The application of the Minimat to plastic fracture: a review." Polymer Testing**6**(Copyright 1986, IEE): 163-187.

Boehme, M. and C. Charton (2005). "Properties of ITO on PET film in dependence on the coating conditions and thermal processing." Surface & Coatings Technology**200**(1-4): 932-935.

Bowen, J. (2010). Instructions for nanoscratching using the AC3100 AFM. D. Compton. University of Birmingham.

Caims, D. R., R. P. Witte, II, *et al.* (2000). "Strain-dependent electrical resistance of tin-doped indium oxide on polymer substrates." Applied Physics Letters**76**(11): 1425-1427.

Cairns, D. R. and G. P. Crawford (2005). "Electromechanical properties of transparent conducting substrates for flexible electronic displays." Proceedings of the IEEE**93**(8): 1451-1458.

Cairns, D. R., D. C. Paine, *et al.* (2001). The mechanical reliability of sputter-coated indium tin oxide polyester substrates for flexible display and touchscreen applications, Warrendale, PA, USA, Mater. Res. Soc.

Cairns, D. R., S. M. Sachsman, *et al.* (2000). "Mechanical behavior of indium oxide thin films on polymer substrates." Materials Research Society Symposium - Proceedings**594**: 401-406.

Cao, L.-R., X.-L. Chen, *et al.* (2009). "Properties of ITO films deposited on PET substrate at low temperature." Guangdianzi Jiguang/Journal of Optoelectronics Laser**20**(5): 628-632.

Colaneri, N. (2010). Arizona State University Flexible Display Centre brochure. Tempe, Arizona. Arizona State University Flexible Display Centre.

Chen, Q., Xu, L., Salo, A., Neto, G., Freitas, G., (2008). Reliability study of flexible display module by experiments, Piscataway, NJ, USA, IEEE.

Cho, S.-W., K.-H. Choi, *et al.* (2008). Characteristics of ITO electrode films grown on PET substrate by roll-to-roll facing target sputtering system for flexible OLEDs, Ilsan, Korea, Republic of, Korean Information Display Society.

Chrisey, D. B. and G. Hubler (1994). Pulsed laser Deposition of Thin Films. USA, John Wiley and Sons.

Crawford, G. P. (2005). Flexible Flat Panel Displays. Chichester, John Wiley and Sons.

Dong-Sing, W., L. Shui-Yang, *et al.* (2006). "Improvement of indium-tin oxide films on polyethylene terephthalate substrates using hot-wire surface treatment." Thin Solid Films**501**(1-2): 346-349.

DuPont Teijin Films 3600 Discovery Drive, Chester, VA 23836 USA.

Eason, R., Ed. (2007). Pulsed Laser Deposition of Thin Films. Southampton, Wiley Interscience.

Ellis, G. (2009). Mechanical Reliability of Flexible Touch Screens and Displays. Undergraduate Research Project, University of Birmingham.

Ellmer, K. (2001). "Resistivity of polycrystalline zinc oxide films: Current status and physical limit." Journal of Physics D: Applied Physics**34**(21): 3097-3108.

Folcher, G., H. Cachet, *et al.* (1997). "Anodic corrosion of indium tin oxide films induced by the electrochemical oxidation of chlorides." Thin Solid Films**301**(1-2): 242-248.

Gorkhali, S. P., D. R. Cairns, *et al.* (2004). "Reliability of transparent conducting substrates for rollable displays: a cyclic loading investigation." Journal of the Society for Information Display**12**(1): 45-49.

Greer, J. A. and M. D. Tabat (1995). "Large-area pulsed laser deposition: techniques and applications." Journal of Vacuum Science and Technology A: Vacuum, Surfaces and Films**13**(3 pt 1): 1175-1181.

Hartnagel, H. L., A. L. Dawar, *et al.* (1995). Semiconducting Transparent Thin Films. London, Institute of Physics Publishing.

Hauk, H. and T. L. Alford (2007). Influence of metal impurity defects on the electrical and optical properties of ITO films on the PEN substrates, Warrendale, PA, USA, Materials Research Society.

Hayes, P. (2009). "Realisation of an electronic paper display." Mundo Electronico(406): 50-52.

Heusing, S., P. W. Oliveira, *et al.* (2008). Development of printed ITO coatings on PET and PEN foil for flexible organic photodiodes, USA, SPIE - The International Society for Optical Engineering.

Jones, R. H. (1992). Stress-Corrosion Cracking. Ohio, USA, ASM International.

Kelly, A. and W. R. Tyson (1965). "Tensile properties of fibre-reinforced metals: copper/tungsten and copper/molybdenum." Journal of the Mechanics and Physics of Solids**13**: 329-350.

Kim, E.-H., C.-W. Yang, *et al.* (2010). "Improving the delamination resistance of indium tin oxide (ITO) coatings on polymeric substrates by O2 plasma surface treatment." Current Applied Physics**10**(3, Supplement 1): S510-S514.

Kim, H., J. S. Horwitz, *et al.* (2001). "Indium tin oxide thin films grown on flexible plastic substrates by pulsed-laser deposition for organic light-emitting diodes." Applied Physics Letters**79**(3): 284-286.

Kroeker, K. L. (2009). "Electronic paper's next chapter." Communications of the ACM**52**(11): 15-17.

Kwok, H. S., X. W. Sun, *et al.* (1998). "Pulsed laser deposited crystalline ultrathin indium tin oxide films and their conduction mechanisms." Thin Solid Films**335**(1-2): 299-302.

Lang, U., N. Naujoks, *et al.* (2009). "Mechanical characterization of PEDOT:PSS thin films." Synthetic Metals**159**(5-6): 473-479.

Lechat, C., A. R. Bunsell, *et al.* (2006). "Mechanical behaviour of polyethylene terephthalate polyethylene naphthalate fibres under cyclic loading." Journal of Materials Science**41**(6): 1745-1756.

Lee, D. Y., G. H. Lee, *et al.* (2009). "Effect of substrate temperature on properties of indium-tin-oxide films deposited on poly(ethylene terephthalate) substrate by DC magnetron sputtering." Japanese Journal of Applied Physics**48**(5 PART 3): 05EC031-005EC034.

Leterrier, Y., L. Boogh, *et al.* (1997). "Adhesion of silicon oxide layers on poly(ethylene terephthalate). I. Effect of substrate properties on coating's fragmentation process." Journal of Polymer Science, Part B (Polymer Physics)**35**(9): 1449-1461.

Leterrier, Y., L. Medico, *et al.* (2004). "Mechanical integrity of transparent conductive oxide films for flexible polymer-based displays." Thin Solid Films**460**(1-2): 156-166.

Lisong, Z., A. Wanga, *et al.* (2006). All-organic active matrix OLED flexible display, USA, SPIE-Int. Soc. Opt. Eng.

Ma, T., Bhusha, B. (2003) Technique Development and Measurement of Poisson's Ratio, Lateral Creep Behavior, and Thermal and Hygroscopic Expansion of Individual Layers in Magnetic Tapes. USA, Journal of Applied Polymer Science

Mark, J. E. (2009). Polymer Data Handbook (2nd Edition), Oxford University Press.

McCollough, G. T., C. M. Rankin, *et al.* (2005). Roll-to-roll manufacturing considerations for flexible, Cholesteric Liquid Crystal (ChLC) display media, Boston, MA, United states, Society for Information Display.

Morris, N. J., K. A. Sierros, *et al.* (2008). Mechanical assisted corrosion: An investigation of thin film components used in flexible optoelectronic applications, Los Angeles, CA, United states, Society for Information Display.

Morton, D., E. Forsythe, *et al.* (2007). "Flexible-display development for army applications." Information Display**23**(10): 18-23.
Murakami, H., T. Oya, *et al.* (2007). Study of influence of under layer on indium tin oxide crystallization, Albuquerque, NM, USA, Society of Vacuum Coaters.
Potoczny, G. (2009). Personal Communcation, University of Birmingham.
Ramji, K., D. R. Cairns, *et al.* (2007). Stress corrosion cracking of patterned indium tin oxide electrodes for flexible displays, Long Beach, CA, United states, Society for Information Display.
Raupp, G. B. (2008). Flexible display center at Arizona State University: a unique industry-government-academic partnership for creating revolutionary information display technology, Piscataway, NJ, USA, IEEE.
Sakka, S. (2005). Handbook of sol-gel science and technology: processing, characterization and applications, Springer.
Salehi, A. (1998). "The effects of deposition rate and substrate temperature of ITO thin films on electrical and optical properties." Thin Solid Films**324**(1-2): 214-218.
Sang Soo, K. (2008). LCD: future prospects and impact on human lifestyle, Piscataway, NJ, USA, IEEE.
Sankir, N. D. (2008). "Selective deposition of PEDOT/PSS on to flexible substrates and tailoring the electrical resistivity by post treatment." Circuit World**34**(4): 32-37.
Seo, S. M., B. G. Kang, *et al.* (2009). "Chromaticity (b*) and transmittance of ITO thin films deposited on PET substrate by using roll-to-roll sputter system." Korean Journal of Materials Research**19**(7): 376-381.
Shin, J. H., S. H. Shin, *et al.* (2001). "Properties of dc magnetron sputtered indium tin oxide films on polymeric substrates at room temperature." Journal of Applied Physics**89**(9): 5199-5203.
Shinar, J. and R. Shinar (2008). "Organic light-emitting devices (OLEDs) and OLED-based chemical and biological sensors: An overview." Journal of Physics D: Applied Physics**41**(13).
Sierros, K. A. and S. N. Kukureka (2007). "Tribological investigation of thin polyester substrates for displays." Wear**263**(7-12): 992-999.
Sierros, K. A., N. J. Morris, *et al.* (2009). "Dry and wet sliding wear of ITO-coated PET components used in flexible optoelectronic applications." Wear**267**(1-4): 625-631.
Sierros, K. A., N. J. Morris, *et al.* (2009). "Stress-corrosion cracking of indium tin oxide coated polyethylene terephthalate for flexible optoelectronic devices." Thin Solid Films**517**(8): 2590-2595.
Sierros, K. A., N. J. Morris, *et al.* (2011). "Spherical indentation and scratch durability studies of transparent conducting layers on polymer substrates." Thin Solid Films, **520**(1): 424-429,
Su, C., T. K. Sheu, *et al.* (2005). "Preparation of ITO Thin Films by Sol-Gel Process and Their Characterizations." Synthetic Metals**153**(1-3): 9-12.
Tarey, R. D., Rastogi, R. S., and Chopra, K. L. (1987). " Characterization Of Thin Films By Glancing Incidence X-Ray Diffraction". The Rigaku Journal 4 (1- 2): 11-15
Thornton, J. A. (1978). Substrate heating in cylindrical magnetron sputtering sources, Switzerland.
Tseng, A. A. (2010). "A comparison study of scratch and wear properties using atomic force microscopy." Applied Surface Science**256**(13): 4246-4252.
Vogels, J. P. A., S. I. Klink, *et al.* (2004). "Robust flexible LCDs with paintable technology." Journal of the Society for Information Display**12**(4): 411-416.
Wei, C. and C.-H. Chen (2008). "The effect of thermal and plastic mismatch on stress distribution in diamond like carbon film under different interlayer/substrate system." Diamond and Related Materials**17**(7-10): 1534-1540.
Weigel, K. and R. Dreyer (2008). "Zinc oxide - Production, market and applications." World of Metallurgy - ERZMETALL**61**(5): 314-317.

Wu, W. F. and B. S. Chiou (1997). "Mechanical properties of r.f. magnetron sputtered indium tin oxide films." Thin Solid Films**293**(1-2): 244-250.

Yang, Y. and X. Zeng (2009). Effects of substrate temperature on properties of the aluminum-doped zinc oxide thin films deposited by RF magnetron sputtering, Wuhan, China, SPIE.

Yip, W. C., A. Gururaj Bhat, *et al.* (1994). Room temperature laser deposited indium tin oxide films for display applications, Pittsburgh, PA, USA, Mater. Res. Soc.

You, Y. Z., Y. S. Kim, *et al.* (2008). "Electrical and optical study of ITO films on glass and polymer substrates prepared by DC magnetron sputtering type negative metal ion beam deposition." Materials Chemistry & Physics**107**(2-3): 444-448.

Yu, X., C. Wang, *et al.* (2006). "Recent developments in magnetron sputtering." Plasma Science and Technology**8**(3): 337-343.

Zhang, S. and N. Ali (2007). Nanocomposite thin films and coatings: processing, properties and performance. London, Imperial College Press.

Zhinong, Y., L. Yuqiong, *et al.* (2009). "Properties of indium tin oxide films deposited on unheated polymer substrates by ion beam assisted deposition." Thin Solid Films**517**(18): 5395-5398.